DEMOCRITUS UNIVERSITY OF THRACE
FACULTY OF HEALTH SCIENCES
SCHOOL OF MEDICINE

ATHENA
RESEARCH AND INNOVATION CENTER IN
INFORMATION COMMUNICATION AND KNOWLEDGE TECHNOLOGIES

Multi-modal Data Acquisition to Inform Artificial Intelligence based Clinical Physiotherapy

MSc THESIS

MSc in

BIOMEDICAL INFORMATICS

Aikaterini Tzatzimaki

Supervisor:
Eleni Kaldoudi
Professor of Medical Physics and Medical Informatics
School of Medicine, Democritus University of Thrace, Greece

ALEXANDROUPOLI, GREECE

MARCH 2026

MSc Thesis

Submitted for the Degree of Master of Science in Biomedical Informatics,

Jointly Organized by the

School of Medicine, Democritus University of Thrace and

ATHENA Research and Innovation Centre in Information Communication and Knowledge Technologies

Multi-modal Data Collection to Inform Artificial Intelligence based Clinical Physiotherapy

by

Aikaterini Tzatzimaki

Supervised by

Eleni Kaldoudi
Professor of Medical Physics and Medical Informatics
School of Medicine
Democritus University of Thrace, Greece

Approved on 28 Μαρτίου 2026 by the Examination Committee:

Eleni Kaldoudi	**Stylianos Didaskalou**	**Aliki Fiska**
Professor School of Medicine, Democritus University of Thrace, Greece	Associate Researcher ATHENA Research and Innovation, Greece	Professor School of Medicine, Democritus University of Thrace, Greece

Μεταπτυχιακή Διπλωματική Εργασία

Υποβλήθηκε για το Πτυχίο Μεταπτυχιακών Σπουδών στην Βιοϊατρική Πληροφορική

που Συνδιοργανώνεται από το

Τμήμα Ιατρικής, Δημοκρίτειο Πανεπιστήμιο Θράκης και

ΑΘΗΝΑ Ερευνητικό Κέντρο Καινοτομίας στις Τεχνολογίες της Πληροφορίας, των Επικοινωνιών και της Γνώσης

Συλλογή Πολυτροπικών Δεδομένων για την Ενίσχυση της Κλινικής Φυσικοθεραπείας με την Χρήση Τεχνητής Νοημοσύνης

της

Αικατερίνης Τζατζιμάκη

Επιβλέπουσα

Ελένη Καλδούδη

Καθηγήτρια Ιατρικής Φυσικής – Ιατρικής Πληροφορικής
Τμήμα Ιατρικής
Δημοκρίτειο Πανεπιστήμιο Θράκης

Εγκρίθηκε στις 28 Μαρτίου 2026 από την Εξεταστική Επιτροπή:

Ελένη Καλδούδη	**Στυλιανός Διδασκάλου**	**Αλίκη Φίσκα**
Καθηγήτρια Τμήμα Ιατρικής, Δημοκρίτειο Πανεπιστήμιο Θράκης	Συνεργαζόμενος Ερευνητής Ερευνητικό Κέντρο ΑΘΗΝΑ	Καθηγήτρια Τμήμα Ιατρικής, Δημοκρίτειο Πανεπιστήμιο Θράκης

Tzatzimaki A., Multi-modal Data Collection to Inform Artificial Intelligence based Clinical Physiotherapy, MSc Thesis, Master of Science in Biomedical Informatics, School of Medicine, Democritus University of Thrace, and ATHENA Research Center, Greece, March, 2026. https://doi.org/10.5281/zenodo.19290578

The author declares that this thesis is his/her own work and to the best of his/her knowledge it:

- Does not breach copyright or other intellectual property rights of a third party.
- Does not contain material previously published or written by a third party, except where this is appropriately cited through full and accurate referencing.
- Does not contain material which to a substantial extent has been accepted for the qualification of any other degree or diploma of a university or other institution of higher learning.
- Does not contain substantial portions of third-party copyright material, including but not limited to charts, diagrams, graphs, photographs or maps, or in instances where it does the author has obtained permission to use such material and allow it to be made accessible worldwide via the Internet as part of this thesis.

During the preparation of this thesis Gemini 3 Flash, March 2026 was used to assist with language refinement, content structuring, and editing support. After using this tool/service, the author reviewed and edited the content as needed and takes full responsibility for the content of the final thesis.

This Thesis was conducted in part within the context of European Union Horizon Europe project ThrombUS+, Grant Agreement No. 101137227. ThrombUS+ is co-funded by the European Union.

The contents of this thesis are solely the responsibility of the author. Approval of this thesis does not necessarily represent the official views of the Examination Committee, the School of Medicine, Democritus University of Thrace, or ATHENA Research and Innovation Center in Information Communication and Knowledge Technologies.

Τζατζιμάκη Α., Συλλογή Πολυτροπικών Δεδομένων για την Ενίσχυση της Κλινικής Φυσικοθεραπείας με την Χρήση Τεχνητής Νοημοσύνης, Μεταπτυχιακή Διπλωματική Εργασία, ΔΠΜΣ Βιοϊατρική Πληροφορική, Τμήμα Ιατρικής, ΔΠΘ και ΑΘΗΝΑ ΕΚ, Αλεξανδρούπολη, Μάρτιος 2026. https://doi.org/10.5281/zenodo.19290578

Κατά τη συγγραφή της παρούσας διατριβής χρησιμοποιήθηκε το εργαλείο τεχνητής νοημοσύνης Gemini 3 Flash, March 2026 ως βοήθημα για βελτίωση της σύνταξης και της δομής του κειμένου και υποστήριξη της επιμέλειας. Μετά τη χρήση του εργαλείου, ο/η συγγραφέας επιμελήθηκε το περιεχόμενο και φέρει την πλήρη ευθύνη για το περιεχόμενο της τελικής εργασίας.

Η διατριβή εκπονήθηκε εν μέρει στο πλαίσιο του έργου ThrombUS+, με αριθμό σύμβασης χρηματοδότησης 101137227. Το έργο ThrombUS+ συγχρηματοδοτείται συγχρηματοδοτείται από την Ευρωπαϊκή Ένωση στο πλαίσιο του προγράμματος «Ορίζοντας Ευρώπη».

Multi-modal Data Collection to Inform Artificial Intelligence based Clinical Physiotherapy

Aikaterini Tzatzimaki

SUMMARY

The rapid evolution of digital health and telerehabilitation has created an urgent need for reliable, high-fidelity systems capable of providing automated and objective motion analysis. This thesis presents the design, development, and technical validation of an infrastructure for the synchronized recording of multimodal motion data during physical rehabilitation exercises.

The proposed system architecture utilizes a custom multi-threaded Python framework to simultaneously manage six Movella DOT inertial measurement units (IMUs) and a dual-camera setup, capturing motion from two distinct viewpoints. By implementing asynchronous data management and a centralized synchronization protocol based on the sensor manufacturer's technical specifications, the platform ensures the precise temporal alignment of high-dimensional kinematic data with video streams. Technical validation of the infrastructure demonstrated a stable and efficient sampling rate of 30 Hz, maintaining a negligible data loss rate of less than 0.004% over extended recording sessions. These metrics confirm the system's reliability for high-precision applications.

The resulting infrastructure serves as a fundamental tool for creating high-quality, structured multimodal datasets. Such datasets lay the groundwork for the development of Artificial Intelligence (AI) models and serious games. These applications enhance home-based rehabilitation monitoring, promoting patient autonomy and reducing the need for the continuous physical presence of a healthcare professional, ultimately making therapy more accessible and personalized.

The complete source code of the developed can be accessed and cloned via the GitHub link: https://github.com/MSc-Biomedical-Informatics-DUTH-ATHENA/2026_TzatzimakiA_Multimodal-Data-Recording-Studiorecording-studio.git

Part of this thesis was published in: Tzatzimaki K, Portokallidis N, Drosatos G, Kaldoudi E, Didaskalou S. A Comprehensive Infrastructure and Methodology for Multi-Modal Data Acquisition to Empower AI-Based Rehabilitation. In Proceedings of the 19th International Joint Conference on Biomedical Engineering Systems and Technologies, 2026, - Volume 3: HEALTHINF, ISBN 978-989-758-802-0, ISSN 2184-4305, pages 269-278. https://doi.org/10.5220/0014351200004070

and announced in: Tzatzimaki K, Portokallidis N, Kaldoudi E, Didaskalou S. Digital Platform to Support Personalized Physical Rehabilitation. 10th Conference of Education and Research in Medicine, Alexandroupoli, Greece, 27-29 March 2026 [in Greek]

Συλλογή Πολυτροπικών Δεδομένων για την Ενίσχυση της Κλινικής Φυσικοθεραπείας με την Χρήση Τεχνητής Νοημοσύνης

Αικατερίνη Τζατζιμάκη

ΠΕΡΙΛΗΨΗ

Η ραγδαία εξέλιξη της ψηφιακής υγείας και της τηλε-αποκατάστασης έχει δημιουργήσει επείγουσα ανάγκη για αξιόπιστα συστήματα υψηλής πιστότητας, ικανά να παρέχουν αυτοματοποιημένη και αντικειμενική ανάλυση κίνησης. Η παρούσα διατριβή παρουσιάζει τον σχεδιασμό, την ανάπτυξη και την τεχνική επικύρωση μιας υποδομής για την συγχρονισμένη καταγραφή πολυτροπικών δεδομένων κίνησης, κατά την εκτέλεση ασκήσεων φυσικής αποκατάστασης.

Η προτεινόμενη αρχιτεκτονική συστήματος χρησιμοποιεί ένα προσαρμοσμένο πλαίσιο Python πολλαπλών νημάτων για την ταυτόχρονη διαχείριση έξι αδρανειακών αισθητήρων (IMU) Movella DOT και μια διάταξη διπλής κάμερας, για καταγραφή της κίνησης από δύο διαφορετικές οπτικές γωνίες. Με την εφαρμογή ασύγχρονης διαχείρισης δεδομένων και ενός κεντρικού πρωτοκόλλου συγχρονισμού βασισμένου στις τεχνικές προδιαγραφές του κατασκευαστή των αισθητήρων, η πλατφόρμα εξασφαλίζει την χρονική ευθυγράμμιση των κινηματικών δεδομένων με τις ροές βίντεο. Η τεχνική επικύρωση της υποδομής κατέδειξε σταθερό και αποτελεσματικό ρυθμό δειγματοληψίας 30 Hz, διατηρώντας ένα αμελητέο ποσοστό απώλειας δεδομένων μικρότερο του 0,004% σε εκτεταμένες συνεδρίες καταγραφής. Αυτοί οι δείκτες επιβεβαιώνουν την αξιοπιστία του συστήματος.

Η υποδομή που προκύπτει αποτελεί ένα θεμελιώδες εργαλείο για τη δημιουργία υψηλής ποιότητας, δομημένων πολυτροπικών συνόλων δεδομένων. Τέτοια σύνολα δεδομένων θέτουν τις βάσεις για την ανάπτυξη μοντέλων τεχνητής νοημοσύνης και ψηφιακών παιχνιδιών (serious games). Οι εφαρμογές αυτές ενισχύουν την παρακολούθηση της αποκατάστασης κατ' οίκον, προάγοντας την αυτονομία του ασθενούς και μειώνοντας την ανάγκη για συνεχή φυσική παρουσία επαγγελματία υγείας, καθιστώντας τη θεραπεία πιο προσβάσιμη και εξατομικευμένη.

Ο πλήρης κώδικας που αναπτύχθηκε στα πλαίσια της διατριβής μπορεί να ανακτηθεί από το GitHub μέσω: https://github.com/MSc-Biomedical-Informatics-DUTH-ATHENA/2026_TzatzimakiA_Multimodal-Data-Recording-Studiorecording-studio.git

Μέρος της παρούσας διατριβής έχει δημοσιευτεί στο άρθρο: Tzatzimaki K, Portokallidis N, Drosatos G, Kaldoudi E, Didaskalou S. A Comprehensive Infrastructure and Methodology for Multi-Modal Data Acquisition to Empower AI-Based Rehabilitation. In Proceedings of the 19th International Joint Conference on Biomedical Engineering Systems and Technologies, 2026, - Volume 3: HEALTHINF, ISBN 978-989-758-802-0, ISSN 2184-4305, pages 269-278. https://doi.org/10.5220/0014351200004070

και έχει ανακοινωθεί στο συνέδριο: Τζατζιμάκη Α, Πορτοκαλλίδης Ν, Καλδούδη Ε, Διδασκάλου Σ. Ψηφιακή Υποδομή για την Υποστήριξη Εξατομικευμένη Φυσικής Αποκατάστασης, 10ο Συνέδριο Εκπαίδευσης και Ερευνας στην Ιατρική, Σχολή Ιατρικής, Δημοκρίτειο Πανεπιστήμιο Θράκης, Αλεξανδρούπολη, 27-29 Μαρτίου 2026

To my sister, my greatest supporter

ACKNOWLEDGMENTS

Completing this MSc thesis has been a deeply rewarding journey, marked by growth and discovery, which would not have been possible without the support of several key individuals.

First and foremost, I would like to express my deepest gratitude to my supervisors, Professor Eleni Kaldoudi and Dr. Stelios Didaskalou, for their mentorship and the unwavering trust they showed me from the very first day. Their continuous guidance provided the foundation for this work. Furthermore, I would like to thank Professor Aliki Fiska for her time, her constructive feedback and for serving as a member of my examination committee.

This thesis was conducted within the framework of the ThrombUS+ EU Horizon project, and I am profoundly grateful for the opportunity to contribute to its clinical and technological goals. It has been a great honor to collaborate with such a distinguished team, and I am thankful for this being my first formal research experience. Beyond the formal guidance, I would like to extend my thanks to the entire ThrombUS+ team for their overall support, technical assistance and the collaborative spirit they shared with me throughout this process.

Finally, I owe a huge debt of gratitude to my family for their unwavering support throughout this journey. Their belief in me has been my greatest motivation and I could not have reached this milestone without them.

CONTENTS

LIST OF FIGURES

LIST OF TABLES

LIST OF ABBREVIATIONS

Abbreviation	Definition
3D	Third Dimension
AI	Artificial Intelligence
BLE	Bluetooth Low Energy
CF	Complementary Filter
CNN	Convolutional Neural Network
DUTH	Democritus University of Thrace
EKF	Extended Kalman Filter
ENU	East-North-Up
GUI	Graphical User Interface
ICF	Informed Consent Form
IMU	Inertial Measurement Unit
IVR	Immersive Virtual Reality
KF	Kalman Filter
LA	Loss and Avoidance
LSTM	Long-Short Term Memory
MAE	Mean Absolute Error
MAS	Modified Ashworth Scale
MEMS	Micro-Electro-Mechanical Systems
ML	Machine Learning
PAE	Peak Amplitude Error
RGB	Red Green Blue
RMSE	Root Mean Square Error
SDI	Strap-Down Integration
SDK	Software Development Kit
SF	Stochastic Filtering
UI	User Interface
UPDRS	Unified Parkinson’s Disease Rating Scale
VTE	Venous Thromboembolism
XFK	XSens Kalman Filter

Chapter 1| Introduction

The systematic study of human motion constitutes a cornerstone of biomechanics, bridging the gap between physical movement and quantitative analysis. Historically, the pursuit of understanding human kinematics has evolved from the early philosophical observations of Aristotle to the sophisticated mechanical studies of Leonardo da Vinci, eventually leading to the photographic evolutions of the 19th century by pioneers like Eadweard Muybridge [1,2]. In the modern era, this field has been transformed by the integration of high-speed digital imaging and micro-electro-mechanical systems (MEMS), which have transitioned motion capture from specialized laboratories into the fabric of everyday clinical practice [3,4]. The ability to accurately quantify joint angles, spatial orientation and a gait parameter is no longer a luxury of high-end research facilities but a fundamental requirement for modern orthopedics, neurology, physiotherapy and sports science.

In contemporary healthcare, the demand for objective motion assessment is driven by the increasing prevalence of musculoskeletal disorders and the necessity for personalized rehabilitation protocols. Traditional gold-standards systems, such as optoelectronic motion capture, offer unparalleled precision but are often confined by significant logistical constraints, including high operational costs, fixed environments and the “white coat effect”, where patients alter their natural movement patterns under observation [5]. These limitations have catalyzed the shift towards wearable sensing technologies, specifically inertial measurement units (IMUs). By leveraging accelerometers, gyroscopes and magnetometers, these sensors provide a portable and cost-effective alternative, enabling continuous monitoring in real-world settings [6]. This transition is particularly critical for the burgeoning field of telerehabilitation, where the objective is to maintain clinical standards of care within the patient’s home environment.

However, the widespread adoption of wearable technology in clinical decision-making is hindered by several technical and procedural challenges that form the core motivation for this research. The reliability of IMU-based data is highly sensitive to sensor-to-segment alignment, soft tissue artifacts and the inherent drift of inertial sensors over time [5]. In a home-based or non-supervised setting, the risk of sensor misplacement by the user can lead to significant data degradation, potentially resulting in incorrect clinical assessments. Furthermore, the integration of multiple-data streams-such as synchronized video and multi-sensor inertial data-presents substantial computational challenges regarding temporal synchronization and real-time visualization. Without robust framework to address these synchronization and calibration issues, the data captured remains a collection of isolated signals rather than a cohesive representation of human movement.

To address these challenges, this thesis details the design and implementation of an infrastructure for high-fidelity motion data acquisition. The proposed system can support up to six Movella DOT sensors and a dual-camera configuration, managed through a custom-developed, multi-threaded, software architecture. This work focuses on ensuring the temporal integrity of data through rigorous timestamp analysis and implementing a user-friendly calibration procedure to align sensor coordinate frames with anatomical segments’ frames. A significant portion of this research is dedicated to a sensitivity analysis that quantifies the impact of sensor misplacement on acceleration signals, thereby establishing a benchmark for the system’s robustness in real world applications. By providing real-time 3D skeletal reconstruction alongside synchronized video feedback, the system aims to offer a comprehensive tool for objective clinical evaluation and support the generation of robust data sets to inform training of machine learning models.

The structure of this thesis is organized to guide the reader through the theoretical, technical, and experimental phases of the project. Following this introductory chapter, Chapter 2 establishes the theoretical foundation, discussing the physics of inertial sensing, orientation representation via quaternions and the

mathematical principles of sensor fusion. Chapter 3 provides a critical review of the current literature, examining the state of-the-art in wearable motion captures the role of artificial intelligence in automated rehabilitation monitoring. The methodological framework, including software architecture and experimental protocols, is detailed in Chapter 4. Additionally, Chapter 5 presents the experimental results, evaluating the system's performance, the efficiency of the graphical user interface, and the statistical findings from the sensitivity trials, concluding with a discussion on the future implications of this work for digital health and rehabilitation. Finally, Chapter 6 provides the conclusions of the study, summarizing the main contributions of this work and suggesting directions for future research to further advance the field of digital health and remote rehabilitation.

Chapter 2| Theoretical Background

2.1. Human motion analysis

Human motion analysis is a multidisciplinary approach that combines observational techniques with sensor-based measurements to evaluate the mechanical and neuromuscular aspects of human movement. By capturing and interpreting data related to joint angles, segment trajectories and muscle activation patterns, it provides insight into the dynamic function of the musculoskeletal system during voluntary or task specific motion [7].

The study of human motion has deep historical roots. Aristotle was among the first to attempt a scientific description of animal movement, while Leonardo da Vinci conducted anatomical dissections and mechanical studies of posture and gait. In the 17th century, Giovanni Borelli applied mechanical principles to muscular action, earning the title "Father of Biomechanics" [2]. In the 19th century, Eadweard Muybridge pioneered photographic motion capture (1878), followed by Etienne-Jules Marey, who introduced chronophotography and pressure-recording shoes. These innovations laid the foundation for stereophotogrammetry and modern gait analysis. The 20th century saw the development of high speed cameras and systems like Vicon, enabling precise 3D motion capture using markers and infrared technology [2].

Initially, motion analysis relied on optical and mechanical systems such as force platforms and video-based tracking. However, these methods were sensitive to lighting, orientation, and environmental conditions [8]. The emergence of Micro-Electro-Mechanical Systems (MEMS) represented a significant technological leap, leading to the development of wearable devices capable of capturing motion data independently of external factors [3].

Sensor technologies evolved into two main categories [8]:

- Rigid (silicon -based) sensors, which include accelerometers, gyroscopes, magnetometers and integrated Inertial Measurement Units (IMUs), forming the core of modern wearable systems due to their robustness, precision and high sampling rates.
- Flexible sensors, which are made from textile-based or polymer materials designed for enhanced comfort and adaptability. These emerging flexible devices operate largely on a resistive principle and expand motion monitoring capabilities to everyday life applications due to superior wearability and conformability.

The rapid development of wearable sensing technologies has enabled human motion analysis to move beyond controlled laboratory environments. Inertial sensing systems have become increasingly important due to their ability to capture motion continuously during natural daily activities. These developments have importantly expanded the potential applications of motion analysis in fields such as rehabilitation monitoring, sports performance evaluation and ergonomics.

In parallel with sensor development, the integration of artificial intelligence (AI) and machine learning (ML) has fundamentally transformed human motion analysis into an intelligent, data-driven discipline. AI-assisted systems now perform automatic classification of movement patterns, segmentation of gait cycles and real time feedback. This integration enables smart, adaptive biomechanical monitoring both within laboratory settings and real-world environments [8].

2.2. IMU fundamentals

Inertial Measurement Units (IMU) are cutting-edge compact devices fundamentally based on the integration of accelerometers and gyroscopes. These core sensors provide critical information regarding linear acceleration and angular velocity, respectively. Recent technological advancements have significantly enriched the capabilities of IMUs, as they now frequently incorporate magnetometers. The addition of magnetometers expands their functionality, allowing them to provide data on the body's orientation relative to the Earth's magnetic field [9].

More specifically:

- The accelerometer measures linear acceleration along the three orthogonal axes (x, y, z). Its operation is based on Newton's second law of motion, where acceleration is inferred from the displacement of a small test mass suspended inside the sensor. Accelerometer data provide two types of information: the static component, corresponding to the projection gravity, which is useful for detecting orientation relative to the vertical axis and the dynamic component, corresponding to motion included accelerations, which is useful for detecting movement intensity and transitions such as walking, jumping or standing still [10].
- The gyroscope measures angular velocity around the three axes, based on the Coriolis effect. It is essential for tracking rotational motion and estimating changes in orientation over time. By integrating the angular velocity, the gyroscope provides relative orientation, however this integration introduces drift errors, as small inaccuracies accumulate over time [11].
- The magnetometer measures the local magnetic field along each axis. Its operation is based on the principle of magnetic materials to align themselves with the field of the Earth's magnetic field. This fundamental physical principle allows the sensor to function as a digital compass, providing a stable reference toward the planet's magnetic north, thus determining the object's precise orientation in space. When used in conjunction with the accelerometer and gyroscope, it allows for estimating the absolute heading relative to the Earth's magnetic north [12].

Each of these sensors provides partial information about motion or orientation. When their measurements are combined through sensor fusion algorithms, the IMUs can reconstruct the full three-dimensional orientation and movement of the body segment they are attached to.

IMU sensors have gained widespread adoption in recent years, across a broad spectrum of applications. Their popularity stems from the combination of three strategic advantages: low cost, compact size and the minimal computational requirements for data processing [9].

These features enable their flexible integration into a multitude of systems, with emphasis on the following specialized scientific and practical domains [13]:

- Rehabilitation and health: They are utilized for the quantitative analysis of patient mobility, the objective monitoring of rehabilitation progress and the detailed assessment of balance and gait.
- Sports and exercise science: They deliver accurate biomechanical data for technique evaluation, performance optimization and recording of load during training and competition.

- Ergonomics: They serve as an essential tool for the objective assessment of posture, the evaluation of working conditions, and the early identification of risks associated with musculoskeletal disorders in professional environments.

In summary, IMUs provide a versatile and efficient means of quantifying human motion, serving as the foundation for modern wearable sensing systems. Their ability to deliver real-time kinematic data under natural movement conditions makes them a valuable tool in both research and applied biomechanics.

Despite their numerous advantages, IMU-based motion analysis systems also present several challenges. Factors such as sensor misalignment, magnetic disturbances and drift accumulation may affect measurement accuracy. For this reason, appropriate orientation representation methods, calibration procedures and sensor fusion algorithms are required to obtain reliable motion estimates.

2.3. Orientation representation and quaternions

In inertial motion tracking systems, accurately determining the orientation of each sensor in three-dimensional space is fundamental to analyzing human movement. This orientation must be defined relative to a global or local reference frame to enable meaningful interpretation of sensor data [14]. Precise orientation estimation is critical for reconstructing limb trajectories and calculating joint kinematics, which underpin biomechanical analysis and rehabilitation applications [15]. To achieve this, several mathematical models have been developed, including Euler angles, rotation matrices and quaternions, each offering distinct advantages and limitations in term of computational efficiency, singularity avoidance and interpretability [16].

2.3.1. Limitations of Euler angles and rotation matrices

Traditional methods for representing orientation, such as Euler angles and rotation matrices, offer intuitive and geometrically grounded approaches but present notable limitations in practical applications.

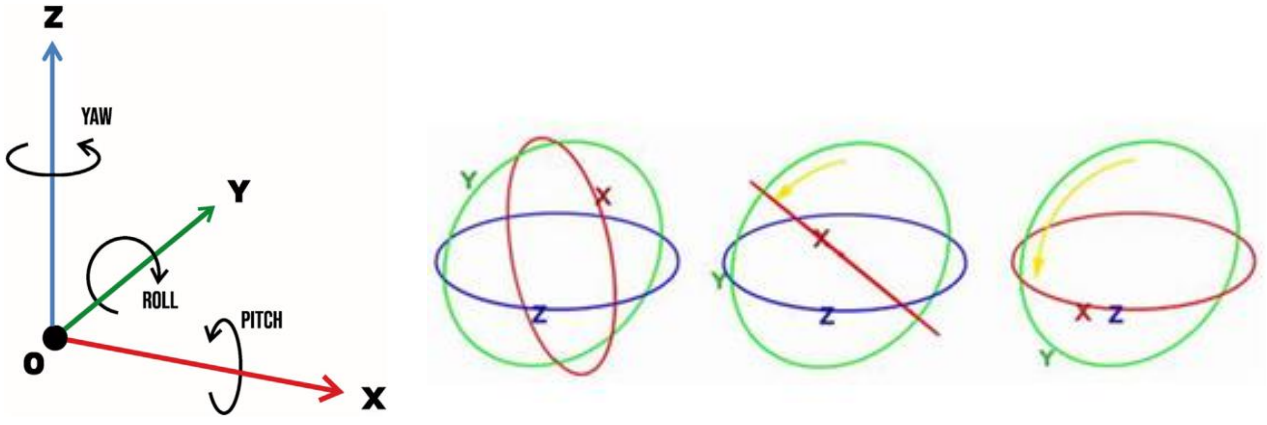

(a) (b)

Figure 1. (a) Representations of Euler Angles showing the three fundamental rotations of a rigid body. Rotation about the X-axis is called pitch, about the Y-axis is roll and about the Z-axis is yaw [18].(b) Illustration of the gimbal lock in a three-axis system. The diagram demonstrates how Euler angle rotations can lead to a loss of a degree of freedom. Left: The initial state where all three axes (X, Y, Z) are independent. Center: A 90^{o} rotation is applied to the Y-axis. Right**:** The resulting "Gimbal Lock" occurs because the X and Z axes have become aligned, reducing the system's maneuverability to two dimensions instead of three [19].

Euler Angles describe orientation through a sequence of rotations around the coordinate axes (typically roll, pitch, yaw), offering an intuitive way to represent 3D orientation (Figure 1a). However, they suffer from the "gimbal" lock (Figure 1b), a singularity that occurs when two rotation axes align, resulting in the loss of one degree of freedom [15]. Moreover, the representation is sensitive to the order of rotations, introducing ambiguity and potential inconsistency in orientation tracking [17].

On the other side, there are the rotation matrices. A rotation matrix $R \in \mathbb{R}^{3X3}$ acts as a mathematical map between two Cartesian coordinate systems: a fixed reference frame (Frame 0) and a rotating body frame (Frame 1) [20]. The 3×3 rotation matrix relating Frame 1 to Frame 0 is defined as shown in Equation [1]:

$$R_1^0 \coloneqq \begin{bmatrix} i_1 \cdot i_0 & j_1 \cdot i_0 & k_1 \cdot i_0 \\ i_1 \cdot j_0 & j_1 \cdot j_0 & k_1 \cdot j_0 \\ i_1 \cdot k_0 & j_1 \cdot k_0 & k_1 \cdot k_0 \end{bmatrix} \in SO(3, \mathbb{R}) \quad [1]$$

Geometrically, the matrix is constructed by taking the unit vectors of the rotating frame (i_1, j_1, k_1) and expressing them as seen from the reference frame (Figure 2). This results in a matrix where each element is a direction cosine, calculated as the dot product between the axes of the two frames. For example, the first column of the matrix represents the coordinates of the body's X-axis relative to the global X, Y and Z axes. Algebraically, these matrices must belong to the Special Orthogonal Group *SO(3)*, meaning they are orthogonal $(R^T R = I)$ and have a determinant of +1 [20].

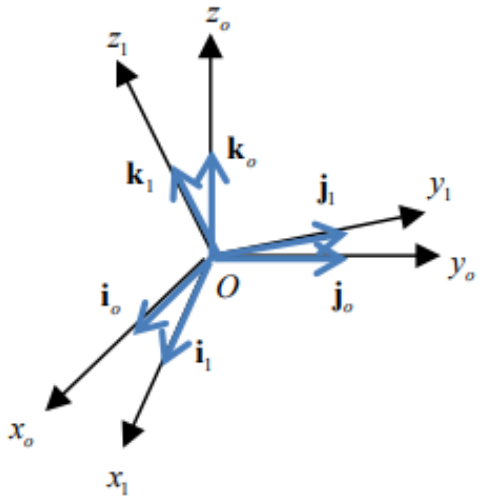

Figure 2. Representation of two Cartesian coordinate frames in 3D space. The diagram illustrates a fixed reference frame (Frame 0) with unit vectors i_o, j_o, k_o and a rotating body frame (Frame 1) with unit vectors i_1, j_1, k_1. The orientation of Frame 1 relative to Frame 0 is defined by the rotation matrix R_1^0, where each column represents the projection of the rotating unit vectors onto the axes of the reference frame using dot products [20].

Nevertheless, they require nine parameters and must satisfy orthogonality constraints, which increases computational burden and can complicate real-time implementation. For real time applications, this redundancy can complicate implementation and reduce numerical efficiency.

2.3.2. Quaternion definition and mathematical formulation

Quaternions offer a compact and robust mathematical framework for representing rotations in three-dimensional (3D) space. A quaternion is defined as a four-dimensional unit vector comprising one real and three imaginary components:

$$q = [w, x, y, z] \quad [2]$$

Alternatively,

$$q = q_0 + q_1\boldsymbol{i} + q_2\boldsymbol{j} + q_3\boldsymbol{k} \quad [3]$$

The imaginary components (i, j, k) follow specific Hamilton product rules, often visualized as a cyclic graph where:

$$i^2 = j^2 = k^2 = ijk = -1 \quad [4]$$

Where w denotes the scalar (real) part, and x, y, z, represent the vector (imaginary) components [21]. For a quaternion to represent a valid rotation, it must satisfy the unit norm condition [21] :

$$\|q\| = \sqrt{w^2 + x^2 + y^2 + z^2} = 1 \quad [5]$$

Based on this norm and the values of the components, several primary types of quaternions are utilized in kinematics:

- Pure Quaternion, where the scalar part is zero:

$$q = (0, q_1, q_2, q_3) \quad [6]$$

- Identity Quaternion, which represents zero rotation:

$$q = (1,0,0,0) \quad [7]$$

- Conjugate Quaternion, which reverses the direction of the vector part:

$$q^* = (q_0, -q_1, -q_2, -q_3) \quad [8]$$

- Quaternion Inverse, defined as

$$q^{-1} = \frac{q^*}{\|q\|^2} \quad [9]$$

To combine two rotations represented by quaternions p and q, the Hamilton product is used. This operation is non-commutative ($pq \neq qp$), meaning the order of rotations is essential. Given $p = (p_0, p_1, p_2, p_3)$ or $p = (p_0, \boldsymbol{p})$ and $q = (q_0, q_1, q_2, q_3)$ or $q = (q_0, \boldsymbol{q})$, the product $r = pq$ is calculated as:

$$r = (p_0 q_0 - \boldsymbol{p} \cdot \boldsymbol{q}, p_0 \boldsymbol{q} + q_0 \boldsymbol{p} + \boldsymbol{p} \times \boldsymbol{q}) \quad [10]$$

2.3.3. From Euler angles to quaternions

The relationship between Euler angles and quaternions can be derived by considering a single rotation around a principal axis. As established in the definition of the rotation matrix, a rotation by an angle ψ around the Z-axis is represented by the elementary matrix R_ψ :

$$R_\psi = \begin{bmatrix} cos\psi & -sin\psi & 0 \\ sin\psi & cos\psi & 0 \\ 0 & 0 & 1 \end{bmatrix} \quad [11]$$

Using the mathematical relationship between the trace of rotation matrix, which is the sum of elements on main diagonal of the matrix, defined as:

$$Trace\ (R) = 2 * \cos\psi + 1 \quad [12]$$

Therefore:

$$|q_0| = \sqrt{\frac{2cos\psi + 1 + 1}{4}} = \sqrt{\frac{1 + cos\psi}{2}} = cos\frac{\psi}{2} \quad [13]$$

$$|q_1| = |q_2| = \sqrt{\frac{cos\psi}{2} + \frac{1 - (2cos\psi + 1)}{4}} = 0 \quad [14]$$

$$|q_3| = \sqrt{\frac{1}{2} + \frac{1 - (2cos\psi + 1)}{4}} = \sqrt{\frac{1 - cos\psi}{2}} = sin\frac{\psi}{2} \quad [15]$$

This results in,

$$q_\psi = cos\frac{\psi}{2} + k\ sin\frac{\psi}{2} \quad [16]$$

Similarly, for the corresponding rotation around the y and x axes:

$$q_\theta = \cos\frac{\theta}{2} + j\sin\frac{\theta}{2} \quad [17]$$

$$q_\varphi = \cos\frac{\varphi}{2} + \iota\sin\frac{\varphi}{2} \quad [18]$$

This representation avoids singularities, supports smooth interpolation between rotations, and simplifies computational operations such as rotation composition. In practical applications, quaternions are favored for real time motion tracking due to their numerical stability and efficiency in combining rotational data from multiple sensors.

2.4. Coordinate systems, alignment and calibration

2.4.1. Global and local coordinate systems

In the context of human motion analysis, the global reference frame is defined as a fixed, right-handed, rectangular Cartesian coordinate system that serves as a universal basis for describing the position and orientation of objects or body segments in three-dimensional space [22]. This frame remains constant in both direction and magnitude, providing a stable and standardized orientation against which all motion-related measurements can be expressed and interpreted.

Typically, the global frame is aligned with the Earth-fixed coordinate system. The z-axis is oriented vertically upward, in opposition to the direction of gravity, while the x-y plane represents the horizontal ground plane. The x-axis is often aligned with the direction of progression, and the y-axis completes the orthogonal triad, ensuring a right-handed system [23,24]. This configuration allows for consistent interpretation of spatial data across different trials, participants and experimental setups.

Complementary to the global frame, each sensor or body segment is associated with a local coordinate system, which is defined relative to the geometry and orientation of the object to which it is attached. These local frames are typically established based on anatomical landmarks or sensor placement, and they move and rotate along with the body segment during motion [23,24]. For example, an IMU mounted on the thigh will record data in its own local frame, which changes dynamically as the thigh moves through space.

Local coordinate system is essential for capturing segment-specific motion characteristics, such as joint angles, angular velocities and segment orientations [7]. However, to analyze whole-body movement or to compare data across segments and subjects, it is necessary to transform local measurements into the global reference frame.

A vector measured in the local frame, v_{local} is transformed to the global frame using a rotation matrix:

$$v_{global} = R_{global<-local}\, v_{local} \quad [19]$$

If the orientation is represented by a quaternion, $q = (w, x, y, z)$,the rotation matrix is:

$$R = \begin{bmatrix} 1-2(y^2+z^2) & 2(xy-wz) & 2(xz+wy) \\ 2(xy+wz) & 1-2(x^2+z^2) & 2(yz-wx) \\ 2(xz-wy) & 2(yz+wx) & 1-2(x^2+y^2) \end{bmatrix} \quad [20]$$

The interplay between global and local coordinate systems is fundamental to biomechanical modeling and sensor fusion techniques. Accurate definition and calibration of both frames are critical for ensuring the validity of motion analysis particularly in applications involving wearable sensors, motion capture systems, or musculoskeletal simulations.

Establishing a clearly defined global reference frame, alongside well-calibrated local coordinate systems, is therefore a prerequisite for accurate, interpretable and scientifically robust motion analysis in both research and clinical applications.

2.4.2. Alignment and sensor-to-segment calibration

Accurate motion analysis using inertial sensors requires not only the estimation of orientation through sensor fusion but also the alignment of each sensor's coordinate frame with the corresponding anatomical segment of the human body [25]. This process, known as sensor to segment calibration, ensures that the orientation estimated by the IMU reflects the actual movement of the limb rather than the arbitrary orientation of the sensor itself [24].

Each IMU measures motion within its own local coordinate system, which is defined by the physical placement of the sensor and may not be aligned with the anatomical axes of the body segment. Consequently, calibration is required to establish a transformation matrix or quaternion that maps the local sensor frame to the corresponding segment reference frame. This transformation allows data from different IMUs to be expressed in a common reference, enabling the accurate reconstruction of joint angles, segment trajectories and kinematic chains.

2.4.3. Calibration approaches

Various calibration approaches have been proposed in the literature to define the transformation between the sensor and the anatomical segment. These can be broadly classified into manual, static, functional and anatomical methods [24]. Each of them presents distinct advantages and limitations depending on the experimental setup and application.

The manual calibration method aims to achieve the most accurate alignment between the sensor's reference frame, and the bone embedded anatomical frame It requires careful placement of each sensor on the appropriate body segment, along with precise alignment to the underlying skeletal structures, to minimize errors across multiple joint angle axes. This accuracy is critical for both single-plane and multi-plane movements, as it enhances the reliability and validity of motion data. In rehabilitation settings, manual calibration is particularly valuable because it provides reproducible results without the need for specialized equipment or complex procedures. Specifically for the elbow joint, manual calibration has been recognized as the preferred approach for general use, offering a practical balance between precision and ease of implementation that supports clinical evaluation and progress monitoring [26].

In static calibration, the subject assumes a known reference pose as an upright standing posture (N-pose) or a seated neutral position, where all body segments are aligned with the global coordinate frame. The orientations measured by the IMUs in this controlled posture are then used to establish the transformation between each sensor's local reference frame and the corresponding anatomical frame. This process provides a consistent baseline that reduces variability and ensures accurate mapping of sensor data to joint kinematics. Because of its simplicity and reproducibility, static calibration has become the most common approach in both commercial motion capture systems and rehabilitation applications. Its efficiency and reliability make it particularly suitable for clinical environments, where standardized procedures and repeatable results are essential for monitoring patient progress [26].

Functional calibration involves performing controlled single-plane movements, such as elbow flexion-extension and pronation-supination, to estimate the relative axis of joint rotation. This approach is particularly advantageous for patients who are unable to maintain a fixed posture, for example those with neurological disorders or posture abnormalities, as it relies on dynamic rather than static alignment [26]. During these functional tasks, the accelerometer is used to determine the orientation of each IMU with respect to the gravity vector, while the gyroscope provides information about the anatomical plane of motion. By integrating data collected from multiple static postures or dynamic tasks, the anatomical axes of each body segment can be reliably estimated in relation to the IMUs. This method therefore offers a flexible and clinically relevant calibration strategy, especially in rehabilitation contexts where patient variability and movement limitations must be accommodated [27].

The anatomical calibration method defines the transformation between sensor and anatomical frames by explicitly referencing palpable anatomical landmarks. In this approach, the examiner identifies bony landmarks on the body segments and uses them to align the sensor axes with the anatomical axes. By anchoring the calibration to skeletal structures rather than arbitrary sensor placement or subject-specific postures, this method reduces soft tissue artifacts and improves the anatomical consistency of joint kinematic estimations. Anatomical calibration has been validated in lower limb and upper-limb motion analysis, showing good agreement with stereophotogrammetry, which is considered the gold standard. Although the procedure requires examiner expertise and can be more time consuming than static or functional methods, it provides enhanced repeatability and accuracy , making it particularly valuable in clinical and research applications where precise anatomical alignment is essential [28].

2.5. Sensor fusion and orientation estimation

Sensor fusion refers to the process of combining data from multiple sensors to produce a more accurate, reliable and stable estimation of physical quantities than would be possible using any individual sensor alone [29]. In inertial motion tracking systems, sensor fusion is primarily employed to estimate the 3D orientation of an object by emerging gyroscope, accelerometer and magnetometer data. This integration compensates for the drift errors inherent in gyroscope data by exploiting the long-term stability of accelerometer and magnetic measurements, resulting in a continuous and drift-free orientation estimate.

The foundation of orientation estimation is the numerical time integration of the differential kinematic equation. This equation describes the relationship between the quaternion derivative and the angular velocity components ($\omega_x, \omega_y, \omega_z$) measured by the gyroscopes [30]:

$$\frac{d}{dt}\overline{\boldsymbol{q}} = \frac{1}{2}[\omega_{ULF}^{T}\,0]^{T} \otimes \overline{\boldsymbol{q}} = \frac{1}{2}\begin{bmatrix} -[\omega_{ULF}\times] & \omega_{ULF} \\ -\omega_{ULF}^{T} & 0 \end{bmatrix}\overline{\boldsymbol{q}} = \boldsymbol{\Omega}\,(\omega_{ULF})\,\overline{\boldsymbol{q}} \qquad [21]$$

Where, $\overline{\boldsymbol{q}} = [\boldsymbol{q}^{T}\ q_4]^{T}$ is the quaternion representing the rotation from the global to the local frame, composed of a vector part q and a scalar part q_4. The term $[\omega_{ULF}\times]$ represents the 3 × 3 skew-symmetric matrix of the angular velocity vector.

2.5.1. Sensor fusion algorithms

In most modern sensor fusion approaches, the unknown orientation variables, such as Euler angles or quaternions, constitute the central object of estimation. This estimation is performed recursively at successive time steps, based on a combination of previous computations and the current sensor readings. Two main categories of algorithms are commonly adopted to achieve this fusion, known as, Complementary Filters (CF) and Stochastic Filters, such as Kalman Filters (KF) [15].

The KF is theoretically considered an ideal algorithm for combining noisy sensor signals to obtain accurate and reliable estimates of system states. Its accuracy stems from the fact that it incorporates known physical properties of the system into the estimation process. In the context of the Stochastic Filtering approach, the filter operates as a recursive prediction -correction model. As illustrated in Figure 3, the KF operates through a recursive prediction-correction cycle. In the prediction step, Equation [21] is utilized for state propagation: the gyroscope's angular velocity measurements are integrated to project the quaternion orientation forward in time. However, to prevent the integration drift inherent in this numerical process, the framework enters a correction step. During this phase, the algorithm incorporates new measurements from calibrated accelerometers and magnetic sensors to refine the a priori estimate [29].

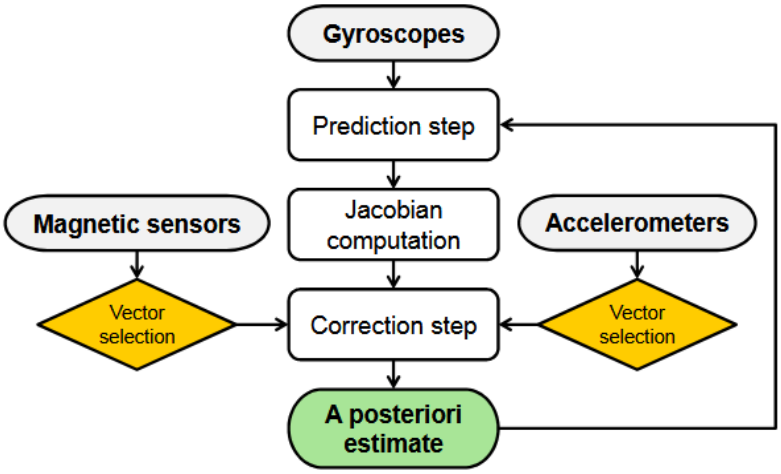

Figure 3. Architecture of a Stochastic Filtering (SF) framework based on the Kalman Filter. The process begins with a prediction step using gyroscope data to estimate the next state. A Jacobian computation is then performed to linearize the non-linear measurement models, followed by a Correction step where Vector selection from magnetic and acceleration sensors is used to refine the estimate. The result is an a posteriori estimate which is fed back into the next recursive cycle to minimize estimation error over time [29].

A defining characteristic of the SF framework is its treatment of sensor reliability. Data confidence is quantified through the standard deviation of measurement noise, which determines the specific weight assigned to each sensor input. By weighing the prediction from Equation [21] against the uncertainty of the aiding sensors, the iterative process reduces high-frequency noise and compensates for long-term drift, thereby enhancing the reliability of kinematic data [29,30]. As a result, the KF has become a cornerstone in robotics, wearable sensor systems, and rehabilitation technologies where accurate real-time motion tracking is essential [31,32]. Their extended version (EKF) for nonlinear models is a well-established method, particularly when complementary filters are developed to blend the data from gyros and the sensors of an aiding system [33].

In high performance commercial systems such as those developed by Movella (XSens), proprietary implementations of the Extended Kalman Filter, such as XSens Kalman Filter (XFK), are employed to integrate accelerometer, gyroscope and magnetometer data for accurate real-time orientation estimation [16].

On the other hand, the complementary filter is a sensor fusion technique widely used in human motion analysis as a computationally efficient alternative to Kalman filtering. They combine information from gyroscopes, accelerometers and magnetometers, exploiting the complementary characteristics of each sensor gyroscopes provide accurate short-term angular velocity but suffer from drift, while accelerometers and magnetometers offer stable long-term orientation references but are more affected by noise.

By blending these signals through a weighted framework (as illustrated in Figure 4), CF based approaches generate reliable orientation and joint angle estimates in real time [34]. Compared to Kalman filter-based methods, CF based estimation has the advantage of reduced computational complexity, requiring only a few tunning parameters, which makes it particularly suitable for embedded and clinical systems [35]. The primary output of this fusion process is a unit quaternion, q, which represents the orientation of the sensor frame relative to the Earth-fixed local frame. This quaternion serves as the operator for the coordinate transformation required to map kinematic data into global reference frame.

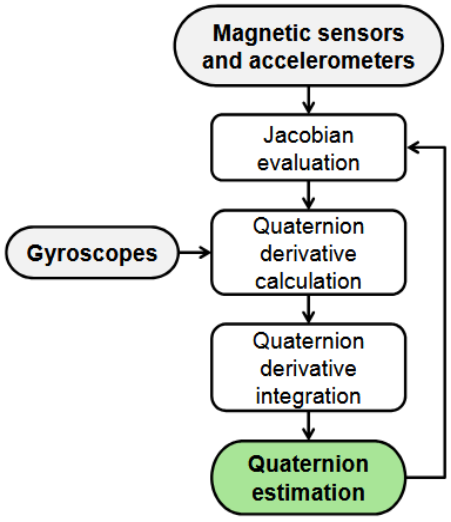

Figure 4. Functional block diagram of a Gradient Descent-based Complementary Filter. The flowchart details the iterative process of quaternion estimation. Raw accelerometer and magnetometer data undergone Jacobian evaluation to determine the orientation gradient via a minimization algorithm. This gradient is fused with the quaternion derivative from the gyroscope, governed by the divergence rate β. The resulting quaternion estimation provides a stable, drift-compensated representation of the sensor's orientation through continuous numerical integration [29].

The CF provides a computationally efficient alternative by extending Equation [21] with an additive correction term. Unlike the EKF, which uses statistical noise modeling, the CF utilizes a single-iteration minimization algorithm to calculate an orientation gradient from the accelerometer and magnetometer data. The primary tuning parameter is the gain β (Equation [22]), which represents gyroscope's measurement errors. It is calculated based on the maximum gyroscope error $\widetilde{\omega}_{max}$ (defined as three times the standard deviation of the gyroscope noise):

$$\beta = \sqrt{\frac{3}{4}}\widetilde{\omega}_{max} \quad [22]$$

Overall, the integration of wearable inertial sensors with advanced orientation estimation algorithms has enabled accurate motion monitoring in a wide range of applications. Nevertheless, the reliability of wearable motion capture systems depends on several factors, including sensor placement, calibration procedures and data processing techniques. Accordingly, recent research has focused on evaluating the performance of wearable systems in clinical and real-world environments, as well as comparing them with established gold-standard motion capture technologies.

Chapter 3| Literature Review

In recent years, the rapid development of wearable sensing technologies has enabled the continuous collection of large volumes of human motion data outside controlled laboratory environments. While IMUs provide detailed kinematic information, the interpretation of these complex datasets requires advanced computational approaches capable of identifying patterns, extracting meaningful features, and supporting clinical decision-making. In this context, Artificial Intelligence (AI) and Machine Learning (ML) techniques have emerged as powerful tools for analyzing wearable sensor data and transforming raw motion signals into clinically relevant information.

Recent research has increasingly focused on the application of AI-based methods to human motion analysis, particularly in the fields of rehabilitation monitoring, gait analysis, and movement assessment. Machine learning algorithms enable the automatic detection of movement patterns, the identification of abnormal motor behaviors and the evaluation of exercise execution quality. These approaches facilitate the objective and quantitative assessment of patient performance, supporting both clinicians and researchers in understanding functional mobility and recovery progression.

The following section reviews studies investigating the use of wearable motion capture systems and artificial intelligence techniques for human motion analysis. Attention is given to clinical applications in rehabilitation, validation studies comparing wearable sensors with established motion capture systems, and emerging approaches that integrate machine learning methods for enhanced motion interpretation.

3.1. Clinical applications of motion capture

Recent literature highlights a significant increase in the use of wearable motion capture systems in clinical settings, as wearables enable the objective evaluation of kinematics in real-world conditions at a lower cost compared to laboratory-based systems. Their capacity for continuous monitoring and ease of integration into daily activities make them particularly suitable for populations requiring long-term or remote monitoring.

In the field of orthopedics and musculoskeletal rehabilitation, IMUs are utilized for assessing range of motion (ROM), gait analysis, and monitoring functional recovery following surgeries such as hip or knee arthroplasty [26–32]. Studies indicate that wearable systems can detect changes in gait symmetry, stability and joint mechanics, providing valuable insights into the progress of treatment and the potential need for adjusting interventions [33]. In neurological disorders such as Parkinson’s disease, multiple sclerosis, and post-stroke rehabilitation, wearables contribute to the recording of motor impairments, the detection of freezing of gait episodes, the assessment of balance, and the measurement of motor fatigue [27]. The ability to record in natural environments allows for the capture of behaviors that often do not manifest in controlled laboratory settings, thereby enhancing the clinical validity of the measurements.

Telerehabilitation is also rapidly growing field, where wearables are used for remote patient monitoring and the provision of real-time guidance. Systems combining IMUs with digital platforms enable the evaluation of compliance, the recording of exercise execution quality, and the adjustment of therapeutic protocols without the physical presence of a therapist [34]. This approach has proven particularly useful for populations with limited access to healthcare services or in cases requiring frequent monitoring.

Furthermore, wearables are widely used in fall prevention and risk assessment for the elderly. Continuous monitoring of mobility, stability and gait patterns allows for the early detection of changes associated with

increased fall risk, supporting interventions aimed at maintaining autonomy. Finally, in the field of sport science, wearable systems are used for technique analysis, training load monitoring and injury prevention. The capacity to record under actual sporting conditions enables the evaluation of parameters that cannot be easily captured in laboratory environments, enhancing the precision of coaching guidance [35].

3.2. Home-based rehabilitation using IMU sensors

Over the last decade, a paradigm shift has been observed in physical therapy, with services increasingly migrating toward home-based models to enhance accessibility and ensure longitudinal care beyond conventional clinical settings. This transition is primarily driven by the clinical non-inferiority of home interventions, meta-analyses have consistently shown that for conditions such as total joint arthroplasty and cardiac recovery, home-based protocols yield functional improvements equivalent to supervised clinical sessions [32,33]. Furthermore, from a socio-economic perspective, shifting the locus of care to the patient's residence significantly reduces the financial burden on healthcare systems while eliminating the logistical barriers and travel costs associated with frequent hospital visits [38].

Despite these clear advantages, the transition to unsupervised environments introduces critical challenges regarding treatment, fidelity and patient safety. In clinical settings, the continuous presence of a therapist ensures that exercises are performed with correct alignment, appropriate speed and the necessary intensity [39]. In contrast, home-based tasks are frequently characterized by compensatory movements or an inconsistent pace, which may compromise the efficacy of the treatment and lead to suboptimal clinical outcomes. This supervision gap often results in a decline in patient motivation and adherence, as the lack of immediate expert feedback creates uncertainty regarding the correctness of the execution and the overall recovery progress.

To address these challenges and bridge the gap between clinical supervision and autonomous recovery, wearable sensing technologies and specifically IMUs, have emerged as pivotal instruments. The most significant contribution of IMUs in this context is the provision of instinctive auditory or visual cues to the patient when movement quality falls below a predefined threshold, thereby preventing the reinforcement of incorrect motor patterns. Recent evidence suggests that such automated feedback systems can effectively substitute into intuitive, actionable instructions for the user [40].

A representative example is the GAMEREHAB@HOME system, which employs a multi-sensor fusion between Kinect cameras and IMUs to animate a 3D avatar and provide high accuracy kinematic data with errors under 5^{o}, for clinical monitoring. Similarly, the HeartHealth platform demonstrates the potential of cloud-based ecosystems for cardiovascular rehabilitation. By utilizing a Motion Evaluation Specific Enabler, this platform records patient movements and compares them against prescribed ground truth recordings, providing both the patient and the healthcare professional with semantic feedback and adherence analytics via a secure web service [41].

Overall, these systems illustrate the growing role of IMU-based technologies in transforming the home environment into a clinically relevant setting for motor recovery. Beyond simple monitoring, wearable sensors enable the objective assessment of exercise execution, support patient adherence, and create the foundation for more interactive rehabilitation approaches that incorporate digital feedback and virtual environments.

Beyond the provision of simple monitoring, recent research emphasizes the role of Immersive Virtual Reality (IVR) and sophisticated gamification dynamics in sustaining long-term engagement. The SPROUTFIT system,

an IVR seed-planting game designed for venous thromboembolism (VTE) prevention, illustrates how the “Loss and Avoidance” (LA) gamification drive can enhance patient effort. By creating a fear of losing accumulated progress or levels, such as the “Master Planter” status, the system significantly increases external regulation and physical exertion, as evidenced by higher heart rates and calorie expenditure compared to non-gamified versions. These interactive digital environments, often paired with wearable sensors to tack lower limb movements, effectively divert the patient’s attention from feelings of fatigue and boredom [42]. Ultimately, these integrated technological frameworks facilitate a granular assessment of exercise execution, transforming the home environment into a clinically validated space for motor recovery.

Beyond the provision of simple feedback, IMUs are increasingly being integrated into interactive digital environments and serious games to address the monotony of repetitive therapeutic exercises. These systems utilize IMU-derived kinematic data to control in-game tasks or animate 3D avatars, rewarding correct execution and encouraging repetition through gamified challenges.

3.3. Artificial intelligence and machine learning for rehabilitation monitoring

The large volume of motion data generated by wearable sensors has created the need for advanced analytical methods capable of extracting meaningful information from raw signals. Artificial Intelligence and Machine Learning techniques have therefore been increasingly applied to rehabilitation data to identify movement patterns, classify therapeutic exercises and evaluate the quality of motor performance. By analyzing kinematic signals collected from wearable devices such as inertial measurement units, machine learning algorithms can support automated assessment of rehabilitation exercises, detection of abnormal movement behaviors and objective monitoring of patient progress. These computational approaches allow rehabilitation systems to move beyond simple signal recording toward intelligent assessment platforms capable of recognizing movement intention, evaluating exercise execution and supporting adaptive therapeutic interventions.

The ability of AI models to detect complex motion patterns from accelerometer and gyroscope data has significantly expanded the potential of wearable technologies for clinical assessment and remote rehabilitation monitoring [43]. These computational techniques enable the transformation of raw inertial signals into actionable clinical insights by identifying intricate motion patterns and extracting meaningful features that characterize human movement [44]. Recent systematic mapping reviews indicate that AI models are increasingly utilized to automate the assessment of exercise quality and to provide objective tracking of patient recovery trajectories in both clinical and home-based settings [45].

A primary application of ML in this domain is the classification of specific motor tasks and the detection of pathological gait patterns, particularly in neurological conditions such as Parkinson’s disease [45]. Advanced deep leaning architectures, such as Convolutional Neural Networks (CNN) and Long Short-Term Memory (LSTM) networks, are frequently employed to analyze time-series data from IMUs, achieving high precision in recognizing movement intentions and classifying rehabilitation exercises [46].

To ensure the technical fidelity of unsupervised rehabilitation, AI frameworks often incorporate synchronization algorithms to match a patient’s real-time performance against expert-defined “ground-truth” templates [47]. These systems can also leverage multi-sensor fusion to animate 3D avatars, providing clinicians with granular kinematic data and ensuring that joint angles are estimated with high accuracy [41].

Kim et al. [48] propose a machine learning approach for grading elbow spasticity stretch testing, offering an alternative to traditional clinician-rated scales. Their findings highlight the potential for remote or non-clinical

monitoring, addressing limitations of conventional MAS-based (Modified Ashworth Scale) evaluations. Han et al., introduces a nonlinear machine-learning model that automatically scores the UPDRS (Unified Parkinson's Disease Rating Scale) gait task using only two shank-mounted IMUs during a shot straight-line walking test. Their approach achieved notably higher accuracy than traditional classifies and produced continuous severity scores, enabling more sensitive monitoring of gait impairment. This low-cost wearable-sensor system demonstrates strong potential for objective, clinically aligned gait assessment in Parkinson's disease [49]. Finally, the synergy of these technologies facilitates the development of virtual assistants for remote rehabilitation integrated into a home-deployable systems, such as the "Virtual-Physio" platform, which provides real-time guidance and ensures clinical fidelity outside traditional settings. [50].

3.4. Data to inform AI-based rehabilitation

The transition from qualitative clinical observation to quantitative, AI-driven rehabilitation requires diverse and synchronized multi-modal data streams. Central to this evolution is the use of optical and video-based data, which facilitates motion capture and non-invasive assessment. These systems process high-resolution RGB (Red-Green-Blue) video streams or depth-map sequences to perform pose estimation, a process where deep learning models identify and track anatomical landmarks in a three-dimensional coordinate system [51]. Based on extracted anatomical landmarks, algorithms can calculate joint angles, limb velocities, and postural alignment without the physical encumbrance of body-worn sensors. The integration of depth-sensing data, often referred to as RGB-D data, provides a volumetric layer that is essential for analyzing spatiotemporal parameters such as step width and center-of-mass displacement, which are critical indicators of balance and fall risk [52]. These optical datasets allow for the identification of subtle compensatory movements and range-of-motion deviations that are frequently imperceptible to the human eye during standard clinical observation.

Complementing these external visual observations, kinematic data harvested from IMUs plays a central role in AI-based rehabilitation, as these sensors capture the dynamic components of movement, such as linear acceleration and angular velocity, which may be too rapid for standard optical frame rates to resolve [53]. When synchronized with optical feeds, this hybrid data approach allows for a 360-degree biomechanical profile, enabling the identification of intricate motion patterns and the classification of specific therapeutic exercises. The resulting feature sets, including stride length, joint angles, and movement velocity, serve as the foundational input for deep learning architectures like Convolutional Neural Networks (CNNs) and Long Short-Term Memory (LSTM) networks [51].

Some studies also include electrophysiological signals that provide insight into the neuromuscular drivers of a patient's physical state. Surface electromyograph data that depicts electrical activity of muscle fibers is utilized to train models to predict movement before it is physically executed [54]. In complex neuro-rehabilitation, these signals may be paired with electroencephalography (data to monitor cortical motor intentions, ensuring that the AI-driven intervention is aligned with the patient's neurological efforts. These physiological and kinematic inputs are often validated against kinetic data to ensure that the AI's assessment of recovery is grounded in the physical forces exerted by the body during movement.

3.5. Data set collection approaches and platforms

The development of robust machine learning models for physical therapy is fundamentally constrained by the complexity of multimodal data acquisition and the subsequent requirement for precise temporal alignment.

A significant number of available datasets focus on optical data alone; a comprehensive systematic review is presented in [56]. Most existing research relies on ad hoc collection setups that are difficult to replicate or scale, often leading to "data silos" where kinematic signals cannot be accurately mapped to the ground-truth visual evidence provided by video recordings.

More recently, research targets the development of multimodal datasets, usually including optical and IMU based data.

In particular, the Multi-Gait and Posture Dataset (2021) is a specialized open-access resource hosted on PhysioNet, designed to support the development of algorithms for gait and posture analysis [57]. It features data from 30 healthy subjects performing various activities, including walking at different speeds and transitioning between different postural states (e.g., sitting to standing). Signals include optical data, IMUs and surface electromyography and were acquired using separate proprietary software, while a custom software-triggering framework was developed to synchronize the different data streams, aligning the 30Hz video with the much faster electromyography and IMU signals.

The KneE-PAD dataset published in 2025 [58] isdesigned for the postural assessment of patients undergoing knee rehabilitation. It features data from 31 participants with various knee pathologies who performed three common lower-limb exercises: squats, leg extensions, and walking. The dataset is unique in that it captures both correct executions and two common "wrong" variations for each exercise, curated from a larger 6-month monitoring study of 267 patients. The primary objective of KneE-PAD is to provide a labeled foundation for training machine learning algorithms to act as "virtual coaches," capable of providing real-time feedback during unsupervised, remote rehabilitation. This dataset features IMU and electrophysiology signals provided by the same integrated sensor and data acquisition was performed by proprietary software.

The FineRehab dataset published in 2024 [59] addresses the "coarse-grained" limitation of existing rehabilitation datasets by providing a much more granular, multi-task approach to movement analysis. While previous datasets often focus on simple exercise classification, FineRehab enables three levels of task analysis: exercise identification, repetition counting, and—most importantly—fine-grained quality assessment (identifying specific errors). It features 50 subjects performing 16 different types of rehabilitation exercises, resulting in a dataset of more than 4000 actions. In this work, the researchers used separate, specialized software ecosystems for each sensor type and implemented a manual synchronization protocol to merge the data afterward.

The K2MUSE dataset published in 2025 [60] introduces a large-scale, multi-modal dataset specifically designed to facilitate the development of lower-limb rehabilitation robots. The dataset includes 30 healthy participants performing 20 different ambulation tasks, including walking at three different speeds and on various inclines. Signals included optical data, electrophysiology and ultrasonography to measure muscle thickness and deformation. The researchers used separate proprietary tools for data acquisition from the various sensors, however they achieved hardware synchronization via a voltage signal that acted as a master signal. Also, they developed several MATLAB (Mathworks Inc.) scripts to create a unified interface for signal collection and saving into a unified format.

The RehabHand (2025) is a multimodal dataset specifically designed to support the automated monitoring and evaluation of hand rehabilitation [61]. This dataset documents 10 individuals performing table-based exercises involving everyday objects like water bottles, balls, and wooden blocks. The dataset includes signals from

wearable cameras and IMUs. Custom Python-based scripts were used post-acquisition to segment, synchronize and package the data.

Despite these significant advancements in multimodal data collection, a persistent gap remains between high-precision laboratory setups and the flexible, unified systems required for practical clinical deployment. While datasets like K2MUSE and MMH-Rehab have moved toward hardware synchronization, they still largely depend on fragmented, proprietary software and complex post-acquisition alignment. There is a critical need for a modular, integrated platform capable of performing real-time, synchronized data collection across diverse sensors within a single software environment. To address this, this thesis presents a unified acquisition platform that integrates dual-camera streams and wireless IMU data. By eliminating the reliance on separate software ecosystems and manual synchronization and integration of data, this research provides the necessary infrastructure for building more responsive and accurate data sets to inform virtual coaches in digital rehabilitation.

Chapter 4| Methodology

4.1. Multimodal data acquisition system overview

The developed system integrates wearable inertial sensors, video acquisition devices and a software platform for synchronized data collection and visualization. An overview of the experimental setup is presented in Figure 5.

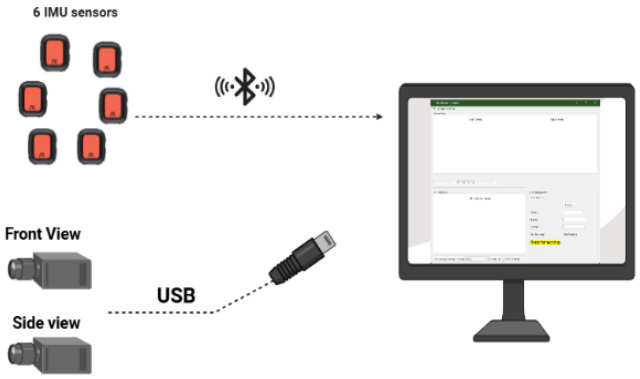

Figure 5. Overview of the experimental setup. Six IMU sensors transmit inertial data wirelessly via Bluetooth to the acquisition computer, while two cameras capture synchronized axial and lateral views of the movement.

The system consists of six wearable inertial measurement units (IMUs) placed on the lower limbs of the participant, two cameras used to record the movement from different viewpoints, and a computer running the *Recording Studio*, a custom-built, Python-based application, which serves as the master controller managing the concurrent data streams from all sources (6 IMUs and 2 cameras). The IMUs transmit motion data wirelessly to the acquisition computer, while the cameras capture front and side views of the performed movement.

Python was chosen because of its widespread use in recent years in the research community. In addition, it provides several specialized libraries for data analysis and signal processing such as the NumPy and Pandas libraries for data management, Matplotlib for graphical representation, and OpenCV for video processing [62-65]. Another important reason is Python's compatibility with the sensor manufacturer's development software (Movella DOT SDK), which facilitates connection and communication with IMU sensors. A comprehensive list of these dependencies, including specific version numbers and instructions for repository access via GitHub, is provided in **Appendix B.**

4.2. Hardware setup for data acquisition system

4.2.1. IMUs technical specifications

Lower-limb motion was captured using wearable inertial measurement units (IMUs) manufactured by Movella Inc., model Xsens DOT, acquired and configured via a systematic process [66]. Each unit is a micro-electromechanical system (MEMS) that integrates a tri-axial accelerometer, tri-axial gyroscope and tri-axial magnetometer enabling the measurement of linear acceleration, angular velocity and magnetic field signals.

These measurements allow the estimation of the orientation and motion dynamics of the body segments they are attached to.

The sensors operate by fusing raw inertial data through an onboard strapdown integration algorithm. The accelerometer measures linear acceleration (including gravity), the gyroscope measures angular velocity and the magnetometer provides a heading reference relative to the Earth's magnetic field. To mitigate common MEMS issues like gyroscope drift, the XSens DOT utilizes an internal Extended Kalman Filter (EKF) to provide stable orientation estimates in the form of quaternion or Euler angles.

Communication between the sensors and the acquisition computer is performed wirelessly via Bluetooth Low Energy (BLE) 5.0 antenna, which ensures high-speed data throughput with lower power consumption. For this setup, the Movella DOT PC SDK 2023.6 was utilized to interface the sensors with the acquisition computer. This SDK , enabling real-time transmission of inertial data without restricting the movement of the participant [16].

The sensor supports sampling rates ranging from 1 Hz to 60Hz [16]. In this study, a sampling rate of 30 Hz was selected for the data acquisition process, which was considered sufficient to capture the dynamics of lower-limb motion while maintaining efficient data handling. While the final Output Data Rate for this study was set at 30Hz, the internal accelerometer and gyroscope sample raw inertial data at 800 Hz. This high-resolution internal clock is critical because it allows the sensor to capture the subtle dynamics and high frequency vibrations of human movement before the data is processed. These raw signals are passed through a Strap-Down Integration (SDI) block, which performs high-speed numerical integration track orientation changes in real-time [13].

The processed inertial data is further refined by the XFKCore, an onboard Extended Kalman Filter (EKF) engine. This engine fuses the highspeed inertial data with the 60 Hz theoretical limit typically required for gait analysis, effectively avoiding aliasing while providing stable orientation estimates in the form of quaternions [13]. The Signal Processing Architecture presented in Figure 6.

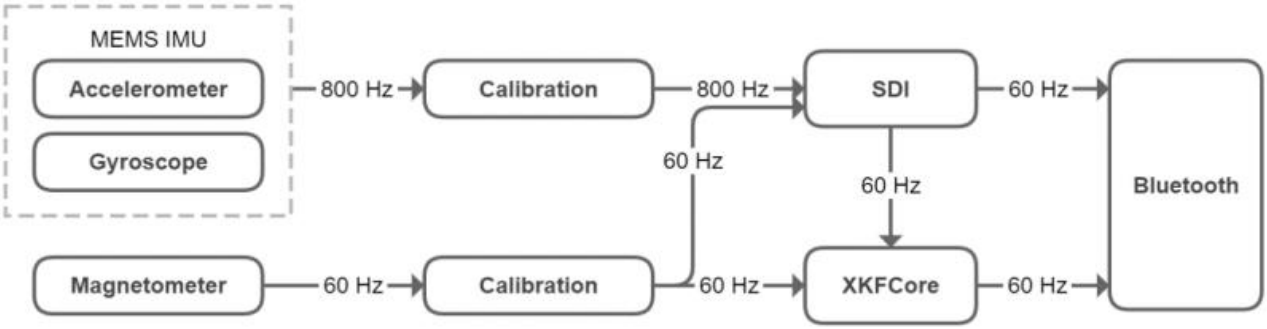

Figure 6. Signal processing architecture of the Movella XSens DOT. The diagram illustrates the internal data flow where the accelerometer and gyroscope sample at 800 Hz, followed by calibration and integration through the Strap-Down Integration (SDI) block. The data is then fused with the 60 Hz magnetometer readings within the XFKCore (Extended Kalm Filter) to provide stable orientation estimates via Bluetooth Low Energy [13].

The main technical specifications of the IMU sensors used in the system are summarized in Table 1.

Table 1. Main technical specifications of the IMU sensors used in the system.

Specification	Value
Sensor model	XSens DOT
Manufacturer	Movella (Xsens)
Accelerometer range	± 16 g
Accelerometer accuracy	0.03 mg
Gyroscope range	± 2000 °/s
Gyroscope accuracy	10 °/h
Magnetometer range	± 8 Gauss
Sampling rate	1 Hz to 60 Hz
Communication protocol	Bluetooth Low Energy

4.2.2. IMUs placement

Movements were recorded using six IMU sensors placed on the lower limbs of the participants. The sensors were attached to the body using adjustable straps, ensuring stable fixation while allowing freedom of movement during the execution of the experimental tasks. Specifically, sensors were positioned on thigh, shank and on the dorsal surface of the foot for both legs. This configuration allows the monitoring of the main lower-limb segments (thigh, shank and foot), enabling the analysis of lower-limb kinematics during movement.

The placement of the sensors is illustrated in Figure 7.

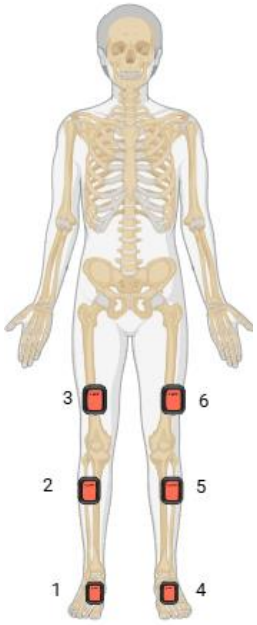

Figure 7. Sensors placement on lower limbs. Sensors were positioned on the anterior mid-thigh, the anterior mid-shank and on the dorsal surface of the foot.

4.2.3. Camera specifications

In addition to the IMU sensors, a camera system was used to capture video recordings of the participant during the execution of the exercises. The video recordings provide visual verification of the performed movements and allow comparison between the sensor-based motion estimation and the actual body posture. Two cameras were used in the experimental setup, positioned to capture axial and lateral views of participants. The main specifications of the cameras are summarized in Table 2.

Table 2. Main technical specification of the cameras used.

Specification	Value
Manufacturer	Creative
Model	Live! Cam V2
Resolution	1080p
Frame Rate	30 fps
Interface	USB-A

4.2.4. Camera positioning

The overall experimental setup and camera placements for the different body postures are illustrated in Figure 8.

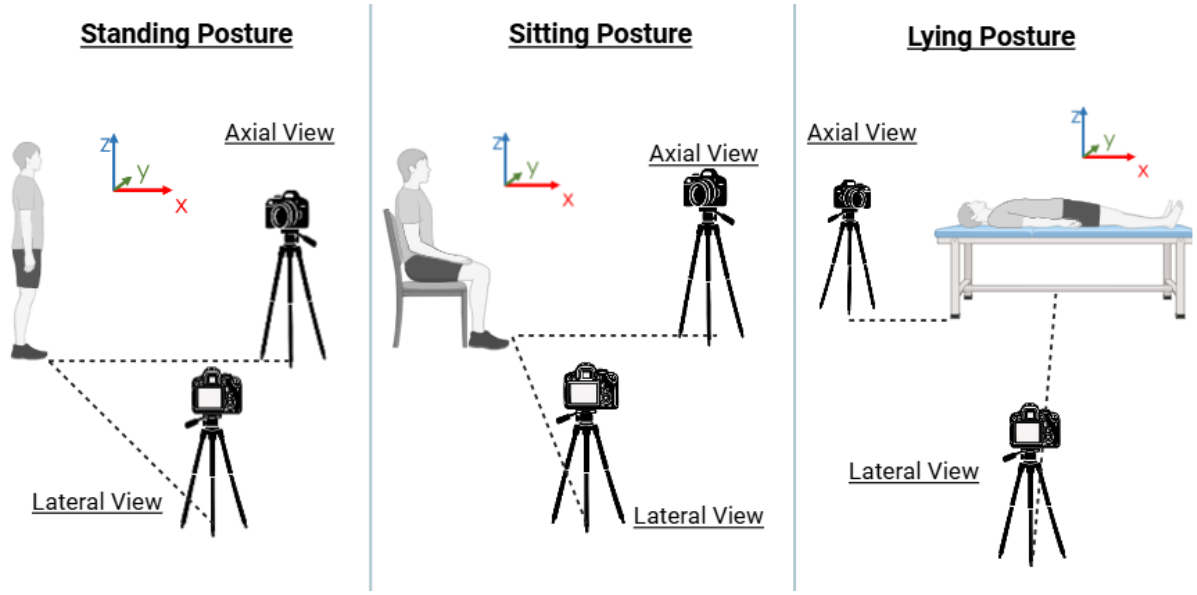

Figure 8. Schematic representation of the camera placement for the different experimental postures. For each posture, two camera viewpoints are used: an axial (frontal) view and a lateral (side) view, enabling simultaneous observation of the participant's movement from complementary perspectives during data acquisition. The X-Y-Z axes indicate the laboratory coordinate system used as the spatial reference frame for motion analysis.

Before each recording begins, a specific preparation procedure is followed. Initially, the six IMU sensors must be placed symmetrically on the patient's lower limbs, specifically on the anterior mid-thigh, the anterior mid-shank and on the dorsal surface of the foot, as mentioned before, using special straps. At the same time, the two cameras are positioned to record the participant's movements from complementary viewpoints. The primary camera is placed in a posterosuperior position relative to the participant, capturing an axial view directed inferiorly (caudally) along the longitudinal axis of the bone. In addition, a second camera is positioned laterally to the participant, capturing a lateral view directed medially toward the body. The exact camera placement is slightly adjusted depending on the participant's posture (standing, sitting or lying). This configuration enables simultaneous visualization of movement from two perspectives and facilitates more accurate interpretation of the recorded motion.

4.3. Software

4.3.1. Overall architecture

The project structure was designed around separate software components, each one is responsible for a specific functionality. An architecture scheme of software is presented in Figure 9. There are three core modules, the IMU Manager which handles communication with the inertial sensors, the Camera Manager which is responsible for controlling the video devices and the File Manager which is responsible for saving all data in an organized and standardized format. These managers operate independently but are orchestrated by the main GUI (Graphical User Interface), allowing for synchronized data acquisition from both modalities.

The core of the inertial data acquisition is the IMU Manager, which is implemented as a replaceable sensor backend to ensure architectural modularity and future scalability. This is responsible for managing the system's inertial sensors, utilizing Movella's provided SDK. Specifically, it automatically searches for and connects Movella DOT sensors, ensuring their accurate synchronization. Through this manager, custom filter profiles are applied, the sampling rate is adjusted, and orientation reset is performed to ensure optimal performance. Finally, it provides real-time sensor data, such as quaternions, acceleration, angular velocity and magnet data, which are available for further processing.

The Camera Manager works alongside the IMU Manager to handle all web camera operations. Using the OpenCV library, it starts up connected cameras and allows specific parameters such as frame rate to be set. Additionally, it supports continuous streaming and video recording during experiments, while ensuring the precise synchronization of each video frame with the data received from other sensors in the system.

All sensor and video data are pushed into a shared queue, which functions as a buffer between the data capture and data saving processes. This queue is a fundamental component for maintaining data integrity and synchronization. By decoupling the data production rate from the consumption rate, the queue prevents any frames or measurements from being lost, which is a common challenge in high- throughput, real- time systems. This buffering strategy is essential for ensuring that the final data set is complete, consistent and perfectly synchronized.

The final stage of the process is File Manager, which is responsible for storing all recorded data in an organized and standardized format. Specifically, it is adapted to create structured files based on variables such as Patient ID, Pose, and Exercise, thus allowing for easy data retrieval and management. Depending on the type of data, different file types are used for storage.

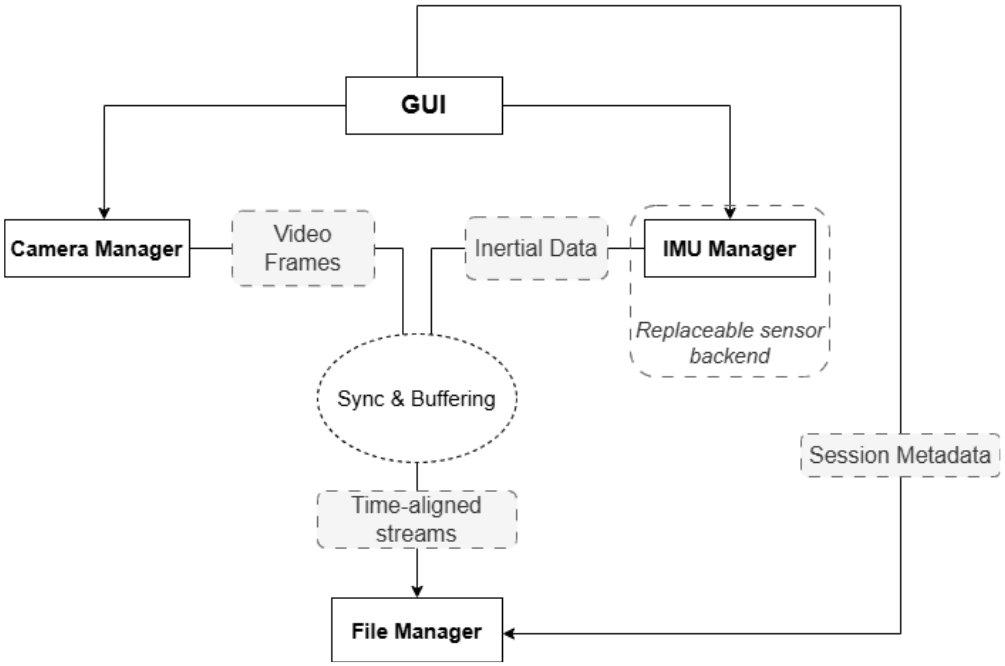

Figure 9. Software high-level architecture and workflow.

4.3.2. Multi-threaded architecture

The application utilizes multi-threaded architecture using *threading.Thread* Python's [67], comprising six dedicated threads. This design approach is critical for preventing bottlenecks and ensuring a high degree of concurrency, as each thread is assigned a specific, non-blocking task. Each thread is responsible for a distinct functional component:

Table 3. Thread explanation.

Thread ID	Function	Used During
Thread 0	Camera 1 streaming	Recording / Streaming
Thread 1	Camera 2 streaming	Recording/ Streaming
Thread 2	IMU Measurement Acquisition	Streaming
Thread 3	IMU 3D Pose plotting	Recording
Thread 4	Camera Figure Updates	Recording
Thread 5	IMU Measurement Acquisition	Recording

A more in-depth analysis of the roles of each thread is as follows:

- **Threads 0 and 1** are dedicated for Webcam Handling. These two are a prime example of parallel processing. By assigning a separate thread to each of the two cameras, the system can capture, process and stream visual data simultaneously. This is particularly important for synchronized data acquisition, as

it ensures that the video frames from both cameras are handled independently, yet without conflict, before being passed to the shares queue.

- **Thread 2** is responsible for IMU Data Preview. The dedicated IMU thread ensures that the data from the sensor is processed and visualized in real time. Because the IMU data stream is continuous and high frequency, a separate thread prevents this task from delaying other critical processes, such as video streaming or user interface updates. This ensures that the user has immediate feedback on the sensor's status.
- **Thread 3** manages the Skeleton Pose Plotting. This thread handles the complex task of dynamically rendering the skeleton pose on the user interface. Plotting this type of data requires significant computational resources. By isolating this function in its own thread, the system avoids any stuttering or freezing on the user interface, thus maintaining a smooth and responsive experience even during intense data processing.
- **Thread 4** is responsible for updating the Camera Figures. The camera views on the GUI must be constantly refreshed to provide live feed to the user. This thread's sole purpose is to handle these UI updates. By separating the UI from the data acquisition and processing threads, the interface remains responsive and fluid, regardless of the load on the rest of the system.
- **Thread 5** is the central mechanism for continuous and uninterrupted monitoring and data collection from IMUs. Its main role is to detect the arrival of new measurement packets in real time, update the latest orientation values, and immediately activate storage or further processing procedures. The use of a time delay mechanism and flag control ensures a smooth flow of information while keeping resource consumption at a controlled level, enabling effective management of system operation.

The control mechanism for each thread is implemented using a flag system, specifically a list of Boolean values named thread_flag. This allows for robust management of the thread lifecycle (start, pause and termination).

4.4. Data source synchronization

According to the Movella DOT User Manual [13] , each sensor operates with its own internal clock domain, which makes time synchronization across multiple devices essential, especially in scenarios where joint calculations depend on signals from more than on IMU. To address this, the Movella DOT system establishes a common sensor time base, to which all devices are aligned after the synchronization procedure. Successful synchronization typically requires about 14 seconds. During this process, one device is designated as the root node while the remaining sensors act as scanners.

The root node periodically transmits advertisement messages, which the scanners receive to estimate the skew and offset of their own clocks and adjust accordingly. To improve synchronization accuracy, the root node is ideally placed in a central position relative to all other sensors. It is important to note that synchronization accuracy decreases over time due to sensor clock drift. As indicated in the manufacturer's specifications, the accuracy degradation is approximately 1 ppm after 30 minutes and 4 ppm after 1 hour.

Synchronization must be performed prior to the start of any measurement session, ensuring that all sensor data streams share a common temporal reference. Once synchronization has been successfully established, multiple measurement trials can be initiated and terminated without the need for additional synchronization procedures.

4.5. Coordinate system and calibration

Each sensor has an internal Sensor Coordinate System defined by the manufacturer and dependent on the physical orientation of the device, as shown in Figure 10. However, for kinematic analysis, these measurements must be expressed relative to a Global Reference Frame. The system utilizes the ENU (East-North-Up) convention, where the Z-axis is aligned with gravity and the Y-axis is aligned with Magnetic North.

To ensure that all six sensors share the directional baseline, A Heading Reset procedure is performed. During this stage, the sensors are placed on a flat, stable surface and aligned in a single direction. This process effectively synchronizes their global orientation, ensuring that "North" is defined identically across the entire sensor network before they are mounted on the participant. This method is applied before placing the sensors on the volunteer. The sensors are activated and placed on a flat, stable surface, aligned in the same direction. [13].

Figure 10. Movella DOT Sensor local coordinate system [13]. The axes are fixed to the physical housing of the tracker, where X follows the longitudinal edge, Y the lateral edge and Z points outward from the sensor's top surface. This local frame is independent of the global Earth-referenced frame (ENU).

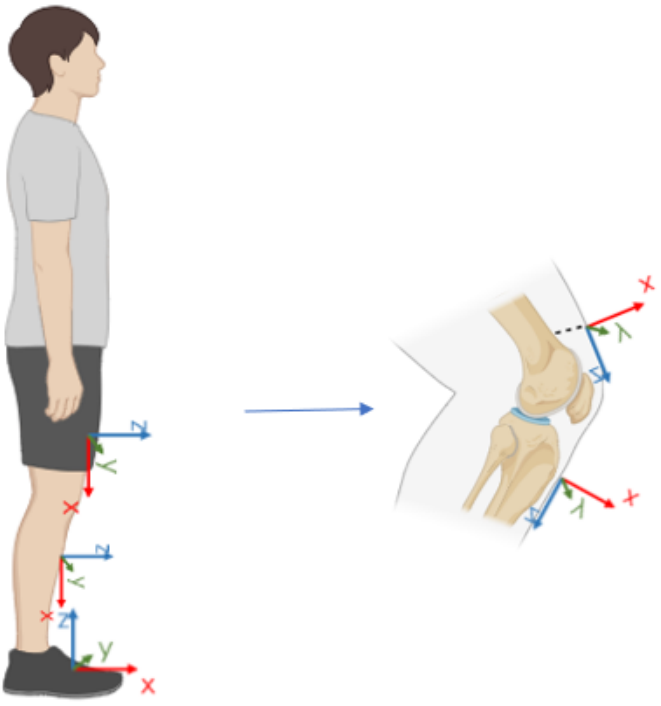

Figure 11. Sensors' coordinate system and misalignment presentation due to soft tissue artifacts.

Once the sensors are attached to the body, a second alignment is required to bridge the gap between the sensor's orientation and the underlying skeletal structure. Because the sensors are placed on the skin and are subject to the contours of muscle and adipose tissue, the Sensor Coordinate System is rarely perfectly aligned with the Anatomical (Bone) Coordinate System (see Figure 11). This discrepancy, known as a misalignment error, is addressed through a functional calibration procedure. By having the participant maintain a predefined static pose the system calculates the offset between the sensor's current orientation and the expected anatomical axis of the bone. This calibration ensures that the digital representation of movement accurately reflects the true biomechanical rotations of the thigh, shank and foot rather than arbitrary tilt of the sensor on the skin surface.

To correct this, once the volunteer is in their initial position (e.g., sitting or standing), Equation [23] is applied to ensure accurate data matching, for all connected IMU sensors individually.

$$q(t)' = q_{calib}^{-1} * q(t) \quad [23]$$

where,

- $q(t)$: the quaternion reading at any given timestamp. It represents the raw orientation of the sensor housing relative to the local earth-fixed frame;
- q_{calib}: the calibration quaternion (or alignment offset). It is calculated at the start of the trial (t=0), when the subject is in the reference pose. It is defined as the inverse of the initial reading, $q^{-1}(0)$. Its role is to "zero out" the arbitrary physical placement of the sensor, mapping the sensor's coordinate system to the intended anatomical axis; and
- $q(t)'$: the calibrated orientation. This is the final output where the sensor data is aligned with the body segment.

4.6. Data flow and storage

Data collection and synchronization are achieved through a common queue, which acts as an intermediate storage space for all incoming data from sensors and cameras. Each recorded measurement includes a timestamp, measurements from the IMUs, and video frames taken simultaneously by two cameras. Final storage is performed by File Manager, which creates files organized based on the details of each experiment, such as Patient ID, Pose, Exercise and Label ID.

The sensor data is recorded in .csv files, where each line corresponds to a unique timestamp and includes synchronized measurements from all sensors. In addition, for compatibility with other platforms, a .txt file is created containing a subset of the data. Finally, the videos collected from the two cameras are stored in .mp4 format.

4.6.1. Generated files and data structure

Data saving is based on locked configuration mapping, which is defined before the recording process begins. To ensure uniqueness and easy identification of each data set, all files are stored with names containing the following information:

- Patient ID
- Pose

- Exercise name
- Label ID
- Trial number
- Timestamp

For example, a typical filename has the following format:

{patient_id}_{pose}_{exercise_name}_{Label_ID}_{trial_number}_{timestamp}.{extension}

4.6.1.1. CSV files

Each line of the .csv file stores the measurements from all IMU sensors at a given moment in time. Each line begins with a main timestamp from the computer system, which serves as the basic reference point for all measurements. This is immediately followed by data from each of the six IMU sensors, from IMU_0 to IMU_5. Also, every sensor has its own independent timestamp, ensuring the exact time of data acquisition. For each sensor, the following are recorded:

- UNIX timestamp
- Sensor timestamp
- The four components of the quaternion (quat.w, quat.x, quat.y, quat.z),
- The three components of acceleration (acc.x, acc.y, acc.z),
- The three components of the magnetic field (mag.x, mag.y, mag.z)
- The pose (Sitting, Lying or Standing)

4.6.1.2. TXT files

During recording, except from .csv file, a .txt file is also created. The .txt file contains the UNIX timestamp and the corresponding measurements from the six IMU sensors for each point in time. This format is simpler than .csv, as it does not include all the individual information, (e.g., magnetic field), but focuses on the necessary data that could be used to reproduce the movement on other platforms or applications.

Each line of the .txt file consists of:

- UNIX timestamp
- The four components of the quaternion (quat.w, quat.x, quat.y, quat.z)
- The four components of the acceleration (acc.x, acc.y, acc.z)
- The four components of angular velocity (ang.x, ang.y, ang.z)

4.6.1.3. MP4 files

Besides the numerical data from the sensors, the system creates also synchronized .mp4 video recordings from the two webcams. Each recording is stored as two video files corresponding to the front and side view, respectively. These recordings provide a visual reference of the movement performed and can be used for visual reference of the movement performed and can be used for qualitative inspection of sensor performance.

The .mp4 files proved valuable for validating the synchronization between video and IMU streams. By visually identifying key events (e.g., foot contact), it was confirmed that the timestamps of the IMU recordings

corresponded accurately with the video frames. Furthermore, the video recordings provided an additional layer of documentation regarding sensor placement and experimental procedure.

4.7. Data logging for system reliability and performance analysis

4.7.1. Timestamp stability analysis

To evaluate the reliability and accuracy of the recorded timestamps, a dedicated analysis was conducted focusing on the consistency of sensor performance under controlled conditions. The experimental procedure involved a single health volunteer, equipped with six IMU sensors placed according to the predefined anatomical configuration outlined in the recording protocol. This standardized placement ensured reproducibility of measurements and minimized variability due to sensor misalignment.

The participant performed one exercise from the proposed physiotherapy routine selected to represent a typical rehabilitation movement with clearly defined phases and expected kinematic patterns. Data acquisition adhered strictly to the established protocol, including consistent sensor attachment, proper calibration procedures, and stable environmental conditions to reduce external sources of noise.

A detailed evaluation of the collection data examined the temporal synchronization between sensors, the stability of timestamp generation and the presence of potential delays or drift during the execution of the movement. Attention was given to identifying discrepancies between expected and recorded event timings, assessing other systematic and random errors. This provided critical insights into the temporal fidelity of the IMU system and its suitability for accurately capturing rehabilitation-related motion tracking.

4.7.2. Sensor placement analysis

To quantify the impact of the sensor misplacement on the accuracy of the recorded acceleration signals, a controlled series of trials was conducted to systematically evaluate how deviations from the correct anatomical placement affect signal quality. In these trials, the IMU sensor on the left thigh was positioned 5cm away from the normal position in three different directions: vertical, inward lateral and outward lateral, as shown in Figure 12.

For each incorrect placement, the resulting acceleration signals were directly compared to those obtained from the correct sensor position. This comparison involved the computation of key statistical error metrics enabling a quantitative assessment of signal deviation. Metrics such as Mean Absolute Error, Root Mean Square Error and Peak Amplitude Error were used to capture both the magnitude and the structural characteristics of the discrepancies between the signals. This approach provided a robust framework for evaluating how sensitive the system is to placement variability.

All measurements were performed with the participant in a standing posture, a condition in which the gravitational component predominantly influences the X-axis of the Movella coordinate system. Under these circumstances, the Y and Z axes primarily reflect dynamic factors such as subtle postural sway and minor voluntary adjustments. This controlled posture allowed for clearer isolation of the effects of senso misplacement, as the expected acceleration patterns are relatively stable and well-defined. Accordingly, deviations introduced by incorrect placement could be more reliably attributed to positional error rather than natural movement variability. The resulting analysis offers valuable insights into the robustness of the IMU-

based measurement system and highlights the importance of precise sensor placement for ensuring accurate motion capture in rehabilitation contexts.

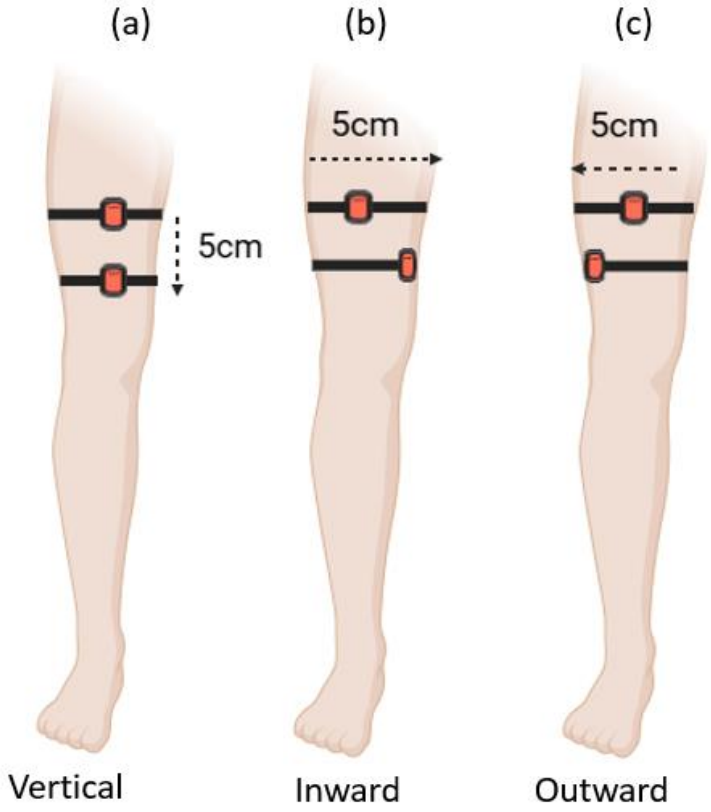

Figure 12. Controlled displacement of the IMU sensor on the thigh during the misplacement experiment. The figure illustrates the experimental configuration used to evaluate the effect of sensor misplacement on the recorded acceleration signals. The IMU sensor was intentionally positioned 5 cm away from its nominal anatomical location on the left thigh in three different directions: (a) vertical, (b) inward lateral and (c) outward lateral, to assess how deviations from the correct placement influence the measured signals.

4.8. Statistical analysis of measurements

The statistical analysis aimed to verify the reliability and consistency of the measurements acquired from the recording system. By processing the collecting time series, we assessed whether the sensors operate synchronously, whether the defined frame rate was respected during acquisition, and whether sensor misplacement introduced measurable deviations.

4.8.1. Data preprocessing

Before proceeding with the statistical analysis, rigorous data preprocessing was implemented to enhance the quality and reliability of the raw data. This protocol addressed several key aspects of the dataset. Initially, the first four samples of each recording were systematically removed. This step was mandatory to mitigate any initial inconsistencies, as preliminary tests revealed that the sensors required a short period to achieve full operational synchronization. Also, the conversion of the IMU timestamps from device specific ticks to milliseconds was performed.

4.8.2. Statistical analysis

4.8.2.1. Analysis of sensor timestamps

For each sensor, the time difference (Δt) between successive time point was calculated. This process allowed the stability of the data acquisition process to be evaluated. Then, based on Equation [24], the average value of Δt was calculated for each sensor, while the minimum and maximum values of Δt were extracted to determine the range of time deviations. The average value confirms whether the sampling rate is close to the nominal value (30 Hz), while the extreme values (Minimum and Maximum) reveal possible momentary delays or sudden changes.

$$\overline{\Delta t} = \frac{1}{N}\sum_{i=1}^{N} \Delta t_i \quad [24]$$

The standard deviation of Δt were extracted to determine the range of time deviations and it was calculating using the Equation [25]. It provides an estimate of the dispersion around the mean value and is therefore a measure of the stability of the sampling rate.

$$\sigma = \sqrt{\frac{1}{N}\sum_{i=1}^{N} (\Delta t_i - \overline{\Delta t}^2)} \quad [25]$$

In addition, the actual sampling frequency was extracted by using Equation [26], to evaluate the consistency of the operating frequency in relation to the nominal value of 30 Hz defined in the application.

$$f_{eff} = \frac{1}{\overline{\Delta t}} \quad [26]$$

Finally, the sample loss rate expressed as a percentage of missing or delayed samples, was estimated to quantify the reliability of the data streams. Dropouts were defined as missing samples or delays exceeding a threshold relative to the expected inter sample interval.

Specifically, when Δt_i was greater than,

$$k * \Delta t_{expected} \quad [27]$$

and

$$\Delta t_{expected} = \frac{1}{f_{nominal}} \quad [28]$$

The nominal sampling frequency ($f_{nominal}$) was set to 30 Hz, corresponding to an expected inter-sample interval of $\Delta t_{expected} = 33\ ms$. Deviations exceeding a threshold relative to this interval were considered as

dropouts. The event was classified as a dropout, where k was set to 1.5. The dropout rate was then calculated according to Equation [29],

$$Dropout\ rate\ (\%) = \frac{N_{drop}}{N_{total}} * 100 \quad [29]$$

In this context, N_{total} denotes the total number of inter sample intervals (Δt) computed from a recording, i.e. one less than the example of raw samples. N_{drop} corresponds to the number of intervals where Δt_i exceeded the dropout threshold.

4.8.2.2. Analysis of acceleration signals

To assess the impact of incorrect sensor placement, the signals resulting from correct and incorrect placements were compared based on a set of statistical metrics. These metrics were calculated for each acceleration axis (x, y, z).

First, the Bias was computed according to Equation [30], to determine whether there was a systematic deviation between the two signals.

$$Bias = \frac{1}{N}\sum_{i=1}^{N}(y_i - x_i) \quad [30]$$

where,

x_i: measurement of the acceleration signal at sample i from the correct sensor placement.

y_i: measurement of the acceleration signal at sample i from the misplaced sensor placement.

N: total number of samples in the analyzed signal.

The Root Mean Square Error (RMSE) was then calculated using Equation [31], providing an overall measure of the error magnitude by combining both systematic and random discrepancies.

$$RMSE = \sqrt{\sum_{i=1}^{n}\frac{(\hat{y}_i - y_i)^2}{n}} \quad [31]$$

The Mean Absolute Error (MAE) was derived using Equation [32], representing the average unsigned difference and thus offering an intuitive indication of the mean deviation.

$$MAE = \frac{1}{N}\sum_{i=1}^{N}|y_i - x_i| \quad [32]$$

Furthermore, the standard deviation of the error calculated according to Equation [33], to quantify the variability of the differences around their mean value, serving as a measure of error stability.

$$\sigma = \sqrt{\frac{1}{N}\sum_{i=1}^{N}[(y_i - x_i) - Bias]^2} \quad [33]$$

Finally, the Peak Amplitude Error (PAE) was determined as the difference between the dynamic ranges (maximum and minimum values) of the two signals, highlighting possible alterations in the motion amplitude caused by misplacement. This was calculated by using Equation [34]:

$$PAE = (\max(y) - \min(y)) - (\max(x) - \min(x)) \quad [34]$$

4.9. Data collection protocol

The data collection workflow follows a rigorous sequence of actions for each participant, according to study protocol [68]. Initially, operators acquire participants demographics, including age, sex, race, alongside body composition measurements such as weight, height, thigh circumference and foot size. Following this, the system is initialized through the Recording Studio application, which provides an integrated list of all required physiotherapy exercises and their corresponding variations. Two web cameras are positioned to capture axial and lateral views, ensuring the field of view captures the full range of motion while maintaining participant anonymity by excluding facial data. After that, six Movella DOT sensors are enabled and connected with the PC.

Once the hardware is secured, a mandatory Heading Reset is performed with the sensors placed parallel to each other to establish a common global reference frame. Next step is sensors' placement symmetrically to the participants lower limbs, as previous mentioned, using elastic straps. This is immediately followed by a functional calibration procedure. During the recording phase, the participant performs a predefined suite of physiotherapy exercises categorized by three body positions: Lying, Sitting and Standing. These exercises such as ankle pumps, heel slides, straight leg raises and mini squats, were specifically selected for their clinical relevance in motor recovery, especially after lower-limb surgery or injury.

For each exercise variation, the operator guides the participant through a three-second countdown to assume the correct starting pose before recording five repetitions. The resulting dataset provides a synchronized output of Inertial data and dual-view video streams. To ensure that dataset is well- structured, each movement is categorized based on the inclusion of a pause (Continuous or Intermittent) and the specific leg involvement (Left, Right, Both). This results in a unique Label ID for every recording, which is automatically embedded into the file metadata.

Chapter 5| Results

5.1. GUI presentation

5.1.1. Main tab

The graphical user interface (GUI) consists of three tabs. The Main Tab provides all the interface functionalities required by the users to operate the system during a recording session. It's built for real-time operation, giving a comprehensive view and full control over the processes, including data streaming and data recording options, with simultaneous live preview of all incoming data (Figure 13).

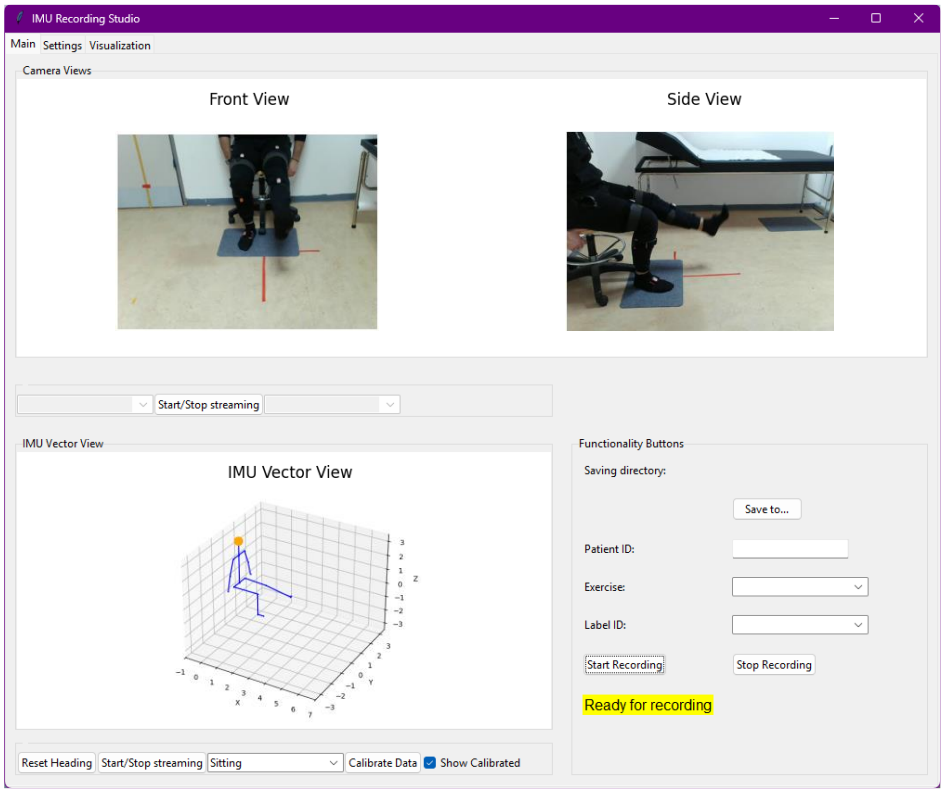

Figure 13. Main Tab of the application interface. The interface integrates synchronized video acquisition and inertial sensor visualization for biomedical data collection. The upper panels display the real-time front and side camera views of the participants during the exercise, while the lower panel presents a 3Dskeletal representation reconstructed from the orientation data of six IMU sensors placed on the lower limbs. The right panel includes controls for configuring the recording session (saving directory, patient ID, exercise type and label) and for starting or stopping the synchronized recording of video and IMU data.

More specifically, two live camera preview windows, showing the axial view and the lateral views, respectively, are positioned in the top side of the window. Both camera previews are updated in real-time during streaming or recording, providing evidence on the recorded field-of-views. On the bottom-left side, the *IMU Vector View* provides a 3D visual representation of the human body, dynamically updating with incoming quaternion data (Figure 14). Below this area, are the buttons which are responsible for: *Reset Heading*, *Start* and *Stop*

streaming buttons, pose selection drop down menu (Sitting, Standing, Lying), as well as the *Calibrate Data* button and *Show Calibration* tick box.

Each of these controls serves a specific function within the system:

- Reset Heading: This button reinitializes the orientation of all connected IMU sensors by resetting their heading to a common reference frame. It is typically used to correct orientation drift and ensure consistency before starting measurement.
- Start / Stop streaming: These buttons control the real-time acquisition of data from both the IMU sensors and the cameras. When streaming is enabled, live data are continuously visualized on the interface without being recorded or stored.
- Pose Selection: This dropdown menu allows the user to define the subject's posture. Based on the selected pose, the system updates the underlying skeletal model and joint configuration used for the 3D visualization.
- Calibrate Data: This button captures the current orientation of the IMU sensors and computes a reference transformation (Equation [23]), allowing subsequent measurements to be expressed relative to this calibrated pose.
- Show Calibration: This checkbox enables or disables the visualization of calibrated data, allowing the user to compare raw sensor output with the calibrated motion representation.

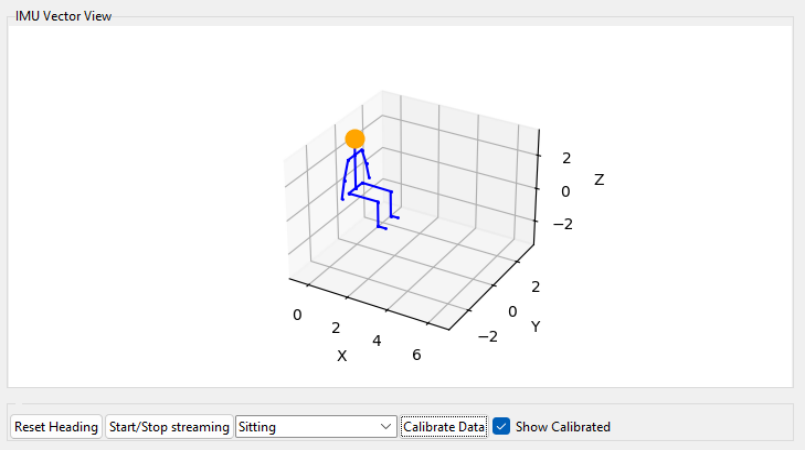

Figure 14. IMU Vector View plot for real-time skeletal visualization. The panel presents a 3-dimensional representation of the lower-body skeletal model reconstructed from the orientation measurements of wearable IMU sensors. The visualization displays the relative orientation of body segments (thigh, calf and foot) while the subject is in a sitting, standing or lying posture, using quaternion data from the sensors to update the joint configuration in real time.

On the bottom-right side of this Main tab, the *Functionality* panel serves as the control center for the recording sessions. From there, the operator can specify the destination folder for saving recorded files, input the Patient ID, and select both the exercise and its variation that the volunteer will perform, choosing from a predefined list. Recording can be initiated or halted using the Start Recording and Stop Recording buttons, respectively. At the bottom of the panel, a status indicator provides real time feedback on system readiness, displaying the message "Ready for recording".

5.1.2. Settings tab

The Settings tab provides comprehensive control over the system's hardware, specifically the cameras and sensors. This interface allows for the precise configuration of each device, ensuring optimal performance for data acquisition (Figure 15).

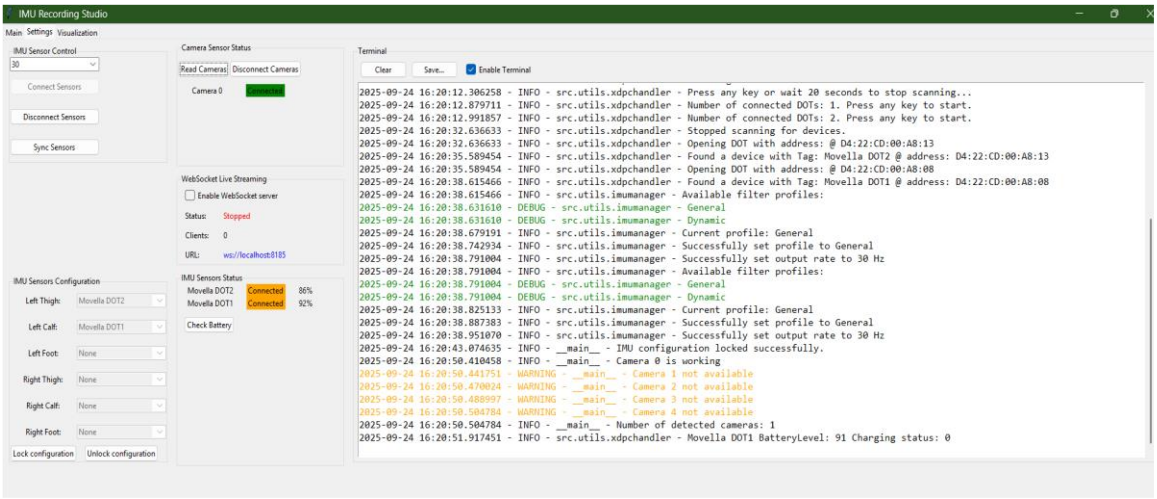

Figure 15. Settings Tab of the Recording Studio interface. This panel allows configuration and monitoring of the data acquisition system before recording. It displays the connection status of the available cameras and IMU sensors, the wireless streaming configuration and a terminal window that reports system messages related to device detection, synchronization and initialization. Additionally, the user can assign each IMU sensor to the corresponding lower-limb body segment to ensure correct sensor mapping prior to data collection.

Located at the top-left of the Settings menu, the IMU sensor control panel allows user to define the sampling frequency of the IMU sensors, and manage connectivity via the *Connect Sensors*, *Disconnect Sensors* and *Sync Sensors* buttons for connecting, disconnecting and synchronizing the IMUs, respectively. Below this panel, in the IMU sensors Configuration panel, the user can assign each connected sensor to a specific leg segment of the lower limbs through which each IMU sensor is assigned to a specific leg segment (e.g., Left Thigh, Left Calf, Left Foot, Right Thigh, Right Calf, Right Foot). The configuration can be locked or unlocked, by using the *Lock* configuration and *Unlock* configurations buttons. Via this approach the users can configure sensor placement based on experimental needs and replace malfunctioning sensors with ease.

In the middle of the Settings tab, the Camera Sensor panel allows the establishment of connection with available camera sensors. In addition, the *Check Battery* button allows us to overview the connected IMU sensors and refresh the charge information. Moreover, the *WebSocket Server* controller ensures interoperability and IMU live-data streaming to other platforms. Finally, on the far right of the screen is a standalone Terminal that displays complete log files, ensuring that the application can operate and be supported independently.

To conclude, the Settings tab brings together all the necessary functions for preparing measurements, by allowing them to check that both the cameras and IMU sensors are connected correctly.

5.1.3. Visualization tab

The Visualization tab is designed to visualize the data collected by the IMU sensors and cameras (Figure 16).

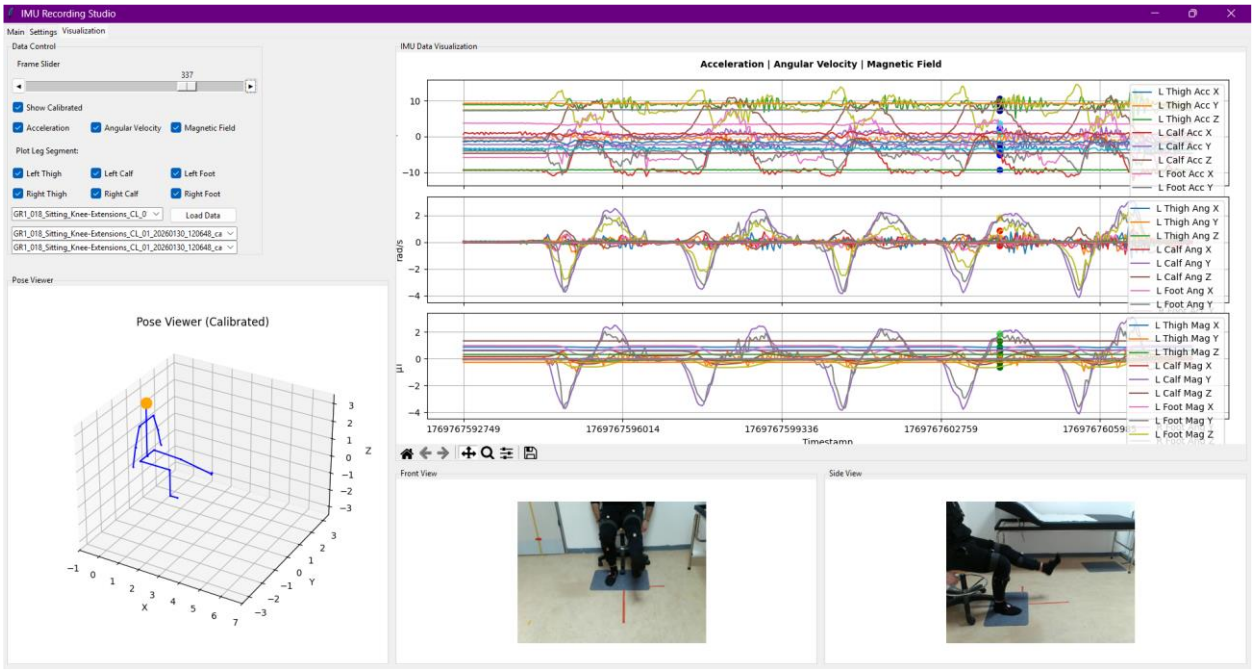

Figure 16. Visualization Tab of the Recording Studio. This panel provides real-time visualization of the acquired data after a recording session. It includes plots of IMU measurements such as linear acceleration and angular velocity, a 3D skeletal representation of the lower-body posture reconstructed from calibrated sensor orientations and synchronized front and side camera views of the participants performing the exercise.

On the bottom-left the *Pose Viewer* section is located, which provides a 3D representation of the skeletal model based on IMU measurements that have been recorded before. On the top-right side of the window in the *IMU Data Visualization* panel, plots of selected signals (e.g., quaternions, accelerations, angular velocities, magnetic fields) for individual body segments are visualized over time. Finally at the bottom-right side of the Visualization Tab, the Front and Side view panels are located, which display the respective frames of the recorded videos by the two cameras, synchronized with the respective sensor data, for the selected time point.

The Visualization tab brings together all visualization capabilities, allowing the researcher to combine sensor data with video and more accurately evaluate the recorded.

5.2. Effect of calibration

To study the need for effective calibration for proper visualization of leg segment orientation, sensors were placed on the lower limbs as described in the methodology, while in lying position. The impact of sensors-to-segment misalignment can be visualized in Figure 17. The figure presents distortions in the leg segment visualization that do not match the reality.

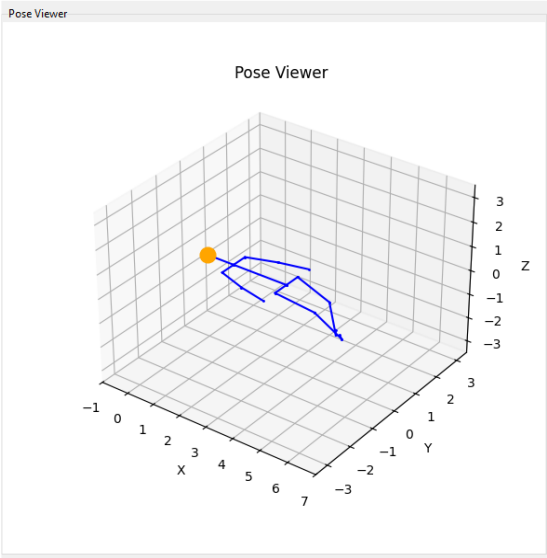

Figure 17. IMU-based skeletal visualization before calibration.

In contrast, Figure 18 illustrates the corrected visualization after applying calibration, with the anatomical axes properly aligned. This demonstrates that the calibration step is required by significantly improving the interpretability and accuracy of the skeletal model.

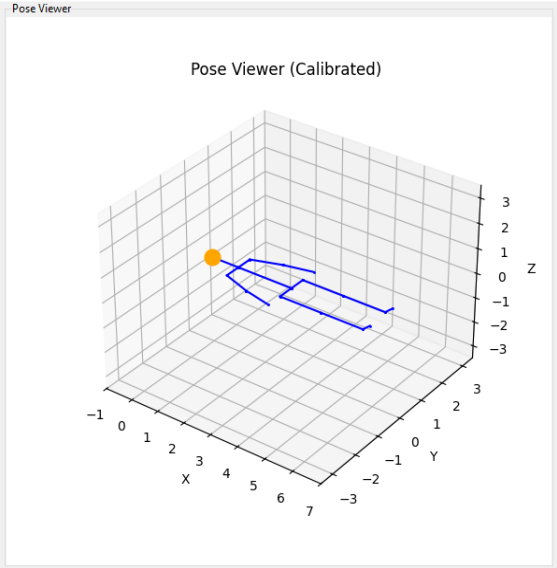

Figure 18. IMU-based skeletal visualization after calibration.

5.3. Statistical analysis

5.3.1. IMU sensors exhibit synchronization consistency during recording

To assess and validate whether sensors operate synchronously and whether the desired frame rate was respected during data collection, statistical processing of recorded timestamps was performed. The analysis and statistical processing of the sensor timestamps yielded the following results, as shown in Table 4.

Table 4. Summary of timestamp analysis metrics for IMU sensors.

IMU ID	Mean Δt (ms)	Standard Deviation (ms)	Effective Frequency (Hz)	Minimum value	Maximum Value	Dropouts (%)
Movella DOT 0	33.42638581	1.752692581	29.91648591	33.3	66.7	0.002771619
Movella DOT 1	33.40787140	2.218178302	29.93306542	0	66.7	0.003325942
Movella DOT 2	33.42638581	2.074847260	29.91648591	33.3	100	0.002217295
Movella DOT 3	33.42638581	1.752692581	29.91648591	33.3	66.7	0.002771619
Movella DOT 4	33.42638581	1.753745443	29.91648591	33.3	66.7	0.002771619
Movella DOT 5	33.44490022	1.920672214	29.89992475	33.3	66.7	0.003325942

More specifically, the evaluation of the inter sample intervals (Δt) recorded by the six Movella DOT sensors revealed a mean value of approximately 33.4 ± 0.5 ms (mean$\pm$SD, n=1437 values per sensor) corresponding to an effective sampling frequency of 29.9$\pm$0.2 Hz, closely aligned with the nominal rate of 30 Hz. The standard deviation of Δt ranged between 1.75 ms and 2.22 ms, indicating stable and reliable sampling intervals.

Although the minimum and maximum values occasionally exhibited outliers (e.g., 0 ms and 100 ms), these instances were rare and did not significantly affect overall performance. Dropout rates remained exceptionally low (<0.004%) across all sensors, further confirming the robustness of the data acquisition process. Collectively, the timestamp analysis demonstrates consistent sensor behavior with minimal packet loss, ensuring high fidelity in temporal signal alignment.

5.3.2. Acceleration analysis

To rigorously examine the impact of sensor misplacement on the accuracy of recorded acceleration signals, a controlled series of experiments was conducted. In these trials, the sensor assigned to the left lower limb was intentionally positioned at various incorrect anatomical locations to simulate misplacement scenarios (see Figure 12).

For each configuration, the acceleration signals captured from the misplaced sensor were systematically compared to those obtained from the correct anatomical placement. This comparative analysis enabled the computation of key statistical error metrics, providing a quantitative assessment of signal deviation resulting from misplacement.

All measurements were performed with the subject in a standing posture, wherein the gravitational vector is expected to align with the X-axis, as defined by the Movella coordinate system (Figure 10). Accordingly, the acceleration signal along the X-axis is primarily influenced by the static gravitational component. In contrast, signals along the Y and Z axes are predominantly shaped by dynamic factors, such as postural sway, subtle balance adjustments, and intrinsic sensor noise, resulting in minor fluctuations that reflect the system's sensitivity to movement.

The outcome of this analysis is detailed in the subsequent tables, which present the quantified error for every misplacement configuration examined.

5.3.2.1. Analysis of the impact of downward sensor misplacement (5 cm)

The results of the impact on downward sensor misplacement are summarized in Table 5.

Along the X - axis, which is dominated by the static gravitational component (g) during the standing pose, Bias is practically zero, while the Root Mean Square Error (RMSE) was 0.045 $\pm$ 0.025 g and Mean Absolute Error (MAE) was 0.042 g values remain low. This shows that the lower placement did not significantly affect the recording of the static component of gravity. The small difference in Peak Amplitude Error (0.054 g) confirms that the range of motion in X-axis was not substantially altered.

Table 5. Error metrics for the case where the sensor on the left thigh was positioned 5 cm below of the nominal anatomical location.

Axes	Bias	RMSE	MAE	Standard Deviation	Peak Amplitude Error
X	0.000000000000000021106711883885	0.045032865	0.042132865	0.024534761	0.0541
Y	0.000000000000000002127667580198	0.039051966	0.030248034	0.034593523	0.0259
Z	-0.000000000000000023040246364974	0.101372191	0.120372191	0.064299617	0.2608

Similarly, the Y- axis, representing lateral dynamic accelerations, exhibits minimal deviations. Bias values are also significant here. The error metrics RMSE was 0.039 $\pm$ 0.020 g and MAE (0.030) suggest negligible differences between signals. The notably low Peak Amplitude Error (0.0259) demonstrates that the lateral component was not substantially altered by the downward displacement of the sensor.

The greatest impact of the misplacement is clearly observed on the Z - axis, which corresponds to the vertical dynamic component. The values of the error metrics are significantly elevated, with RMSE at 0.101 $\pm$ 0.064 g, MAE at 0.120 g and a particularly high Peak Amplitude Error (0.261 g). This phenomenon is likely attributed to the fact that the lower placement positions the sensor closer to areas with increased soft tissue movement on the thigh. Therefore, small movements of the soft tissue or skin deformation are amplified, leading to a greater alteration of the vertical acceleration signal.

5.3.2.2. Analysis of the impact of inward lateral sensor misplacement (5 cm)

The results of the impact on inward sensor misplacement are summarized in Table 6.

Despite practically zero Bias, the error metric values on the X axis are relatively elevated, with RMSE = 0.104 $\pm$ 0.083 g and MAE = 0.068 g. The increased standard deviation indicates greater variability in the recorded signal compared to the reference condition. This suggests that lateral displacement slightly alters the sensor orientation relative to the vertical axis, potentially introducing small angular misalignments that affect the gravity-related component. The high Peak Amplitude Error (PAE= 0.379 g) confirms the significant distortion of the recorded range along the X-axis.

On the y- axis, the Bias remains essentially zero. Although the RMSE value appears low (0.006 $\pm$ 0.090 g), the MAE (0.066 g) and the relatively high Standard Deviation (0.090) indicate the presence of non-systematic deviations and increased dispersion in the signal differences. In addition, the Peak Amplitude Error (0.534 g)

is particularly high, suggesting that the lateral displacement significantly modifies the range and maximum value of the recorded lateral acceleration.

Table 6. Error metrics for the case where the sensor on the left thigh was positioned 5 cm to the right (inwards) of the nominal anatomical location.

Axes	Bias	RMSE	MAE	Standard Deviation	Peak Amplitude Error
X	-0.000000000000000005282460571977	0.104249854	0.067649854	0.083136731	0.3788
Y	-0.000000000000000001572276484582	0.005541691	0.066358309	0.089622743	0.5336
Z	-0.000000000000000002602388664136	0.242949563	0.198149563	0.30691868	0.938

The largest deviations are found on the Z-axis, which proves to be the most sensitive. The error metrics are quite high with RMSE = 0.243 $\pm$ 0.307 g and MAE = 0.198 g. The corresponding Peak Amplitude Error reaches its maximum values (0.938 g), demonstrating that the lateral displacement critically affects the recording of the vertical component.

5.3.2.3. Analysis of the impact of outward lateral sensor misplacement (5 cm)

The results of the impact on inward sensor misplacement are summarized in Table 7.

Despite the Bias remaining virtually zero, the X-axis exhibits elevated error metrics. The RMSE =0.074 $\pm$ 0.057 g and MAE= 0.058 g. These values are higher than those observed in the downward displacement scenario but slightly lower than those reported in the inward displacement case. The Peak Amplitude Error (0.457) suggests a noticeable distortion in the recorded signal amplitude along the axis.

Table 7. Error metrics for the case where the sensor on the left thigh was positioned 5 cm to the left (outwards) of the nominal anatomical location.

Axes	Bias	RMSE	MAE	Standard Deviation	Peak Amplitude Error
X	-0.000000000000000072970460254080	0.073503207	0.057803207	0.057367601	0.4574
Y	-0.000000000000000001294720728426	0.078750146	0.050549854	0.147739335	1.4364
Z	-0.000000000000000050066850568227	0.131481633	0.181681633	0.140133462	0.505

On the Y-axis, this configuration yields the most severe disruption among all tested scenarios. RMSE (0.079 $\pm$0.148 g) and MAE (0.051 g) are notably high. The Peak Amplitude Error reaches 1.436, indicating a substantial alteration in the recorded lateral acceleration amplitude and demonstrating that outward sensor misplacement significantly affects the accuracy of lateral motion measurements.

The Z-axis also reflects considerable deviations, with RMSE = 0.131 $\pm$ 0.140 g and MAE = 0.182 g. The Peak Amplitude Error of 0.505, although lower than that observed in the inward displacement case, remains

significant. These findings confirm that the vertical acceleration component is sensitive to lateral sensor misplacement and continues to exhibit notable distortions under outward displacement conditions.

5.4. Lower limb activity data collection study

To demonstrate the practical utility and robustness of the developed infrastructure, a pilot data acquisition study was conducted. The study is a single-center observational, non-significant risk, training data collection study, conducted in accordance with the principles of the Declaration of Helsinki. The protocol received formal approval from the Research Ethics and Deontology Committees of the Democritus University of Thrace (DUTH) and the ATHENA Research and Innovation Center, protocol numbers: DUTH Ethics Committee ΔΠΘ/ΕΗΔΕ/55711/478, and ATHENA Ethics Committee 54-29/04/2025, respectively. All participants are fully informed about the study's objectives and provide a signed Informed Consent Form (ICF) before any measurements are taken.

As of the current phase of the study, the repository contains synchronized data from the first 28 healthy volunteers toward the final target of 60. Demographic data of the registered participants, specifically illustrating at Figure 19 and Figure 20. The participants performed a comprehensive protocol of 59 commonly prescribed physiotherapy exercise variations, categorized by posture: supine, sitting, and standing. To ensure the resulting dataset captured sufficient intra-subject variability for future AI training, each exercise was performed for five repetitions. This deployment phase successfully generated a multi-modal dataset comprising approximately 6,900 synchronized files, validating the system's capacity for high-volume, synchronized data collection in a clinical context.

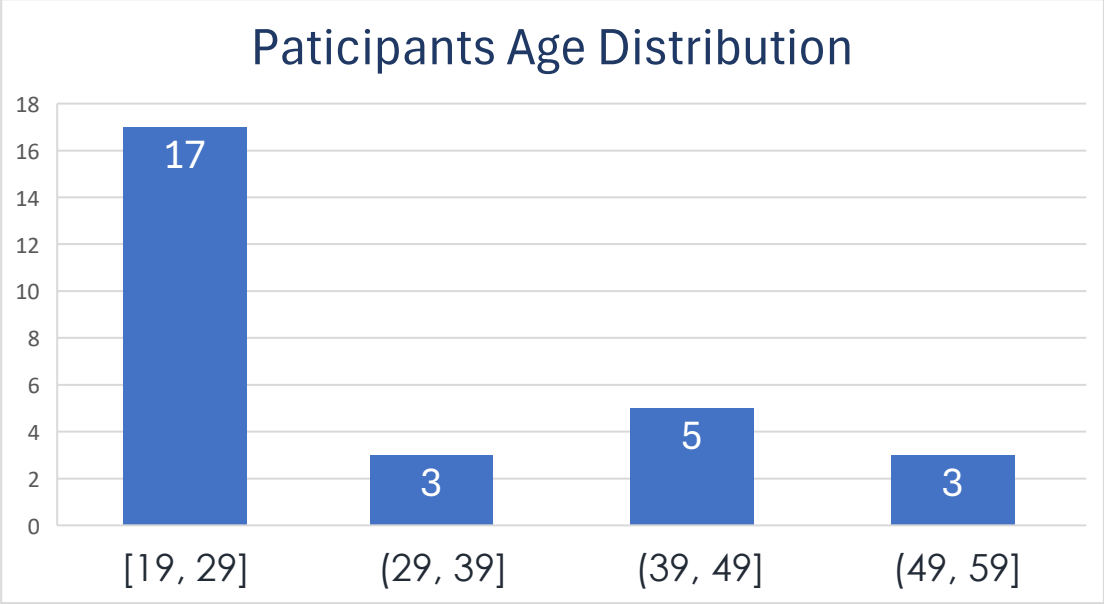

Figure 19. Age distribution of healthy volunteers. The histogram illustrates the demographic profile of the 28 participants currently recorded in the clinical study. While most of the cohort (17 participants) falls within the [19, 29] age bracket, the inclusion of volunteers up to 59 years old ensures a diverse range of motion patterns for the development of robust AI models.

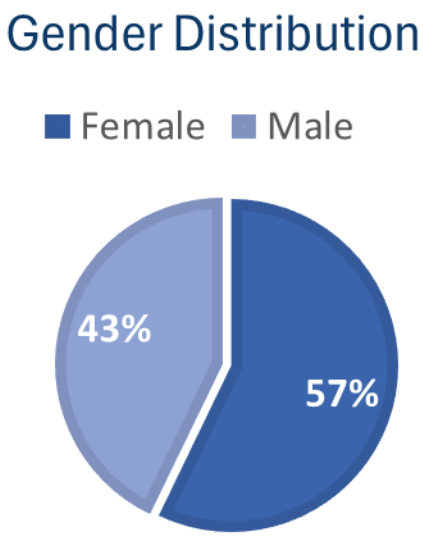

Figure 20. Gender distribution of clinical study participants. The pie chart presents the gender composition of the 28 healthy volunteers recorded to date. The sample consists of 57% female and 43% male participants, indicating a balanced representation that supports the generalizability of the motion recognition models being developed.

Chapter 6| Conclusions and Future Work

The infrastructure and methodology presented in this thesis established a robust foundation for synchronized multimodal motion capture, specifically designed for the rigorous requirements of clinical research and model training. By integrating wearable inertial sensors and a dual-camera setup within a custom muti-threaded Python architecture, the system ensures reliable synchronization, accurate sensor-to-segment calibration and real-time 3D skeletal visualization. Technical validation confirmed that the system maintains high-quality data streams with an effective sampling frequency of 30 Hz and a negligible dropout rate of less than 0.004%. Finally, as part of the system's evaluation, the impact of sensor misplacement on acceleration signals was also studied to quantify signal sensitivity and robustness.

These experimental results, alongside the core technical infrastructure were presented at the 19th International Conference on Health Informatics (HEATHINF 2026) and published in the respective peer-reviewed proceedings. This external validation underscores the novelty of the synchronized acquisition framework and its potential to serve as a standardized tool for objective, data driven physical therapy and clinical decision making [69].

Building upon the technical validation of the acquisition infrastructure, specifically regarding synchronization stability and robustness, future work will focus on expanding the software's capabilities to bridge the gap between raw data acquisition and automated clinical insight. A key priority will be the full quantitative validation of cross-modal synchronization between the IMU sensos and the camera streams. This will involve frame-level temporal alignment analysis, controlled synchronization experiments, and a systematic estimation of inter-stream latency to further strengthen the temporal coherence of the generated multimodal datasets.

In parallel with these technical refinements, there are plans to integrate advanced data labeling and annotation features directly within the Recording Studio platform. By enhancing the software infrastructure to support the creation of high-quality, structured datasets, the system will facilitate the robust training of Machine Learning models. These enhancements are intended to enable the automatic recognition of specific rehabilitation exercises and movement pattens, serving as the backbone for intelligent, adaptive feedback systems designed to provide personalized therapy.

The developed infrastructure serves as the foundation for a comprehensive AI-based rehabilitation pipeline. This conceptual framework begins with high-quality multimodal data acquisition to provide the synchronized datasets necessary for model development. Once trained, these models will be integrated into both clinical and home-based deployments, such as serious games and extended reality (XR) environments, creating a feedback-driven system that supports continuous model refinement and personalized patient care.

Finally, clinical data collection is currently underway to support these objectives. The software platform is being deployed in clinical settings to record rehabilitation exercises performed by patients under standardized protocols. This growing repository will be instrumental for future research, enabling comprehensive analysis of inter-subject variability. Ultimately, these clinical datasets will provide the necessary foundation for the development, training and rigorous evaluation of AI models aimed at enhancing rehabilitation support and assisting in clinical decision-making.

References

1. Baker R. The history of gait analysis before the advent of modern computers. Gait Posture. 2007 Sep;26(3):331–42. doi:10.1016/j.gaitpost.2006.10.014 PubMed PMID: 17306979.
2. Lu T, Chang C. Biomechanics of human movement and its clinical applications. The Kaohsiung J of Med Scie. 2012 Feb;28(2S). doi:10.1016/j.kjms.2011.08.004
3. Aggarwal P, Syed Z, Niu X, El-Sheimy N. A Standard Testing and Calibration Procedure for Low Cost MEMS Inertial Sensors and Units. The Journal of Navigation. 2008 Apr;61(2):323–36. doi:10.1017/S0373463307004560
4. Gu C, Lin W, He X, Zhang L, Zhang M. IMU-based motion capture system for rehabilitation applications: A systematic review. Biomimetic Intelligence and Robotics. 2023 Jun 1;3(2):100097. doi:10.1016/j.birob.2023.100097
5. Villa G, Cerfoglio S, Bonfiglio A, Capodaglio P, Galli M, Cimolin V. Validation of a Commercially Available IMU-Based System Against an Optoelectronic System for Full-Body Motor Tasks. Sensors. 2025 Jan;25(12):3736. doi:10.3390/s25123736
6. Sun Z, Ke Q, Rahmani H, Bennamoun M, Wang G, Liu J. Human Action Recognition From Various Data Modalities: A Review. IEEE Transactions on Pattern Analysis and Machine Intelligence. 2023 Mar;45(3):3200–25. doi:10.1109/TPAMI.2022.3183112
7. Cappozzo A, Della Croce U, Leardini A, Chiari L. Human movement analysis using stereophotogrammetry: Part 1: theoretical background. Gait & Posture. 2005 Feb 1;21(2):186–96. doi:10.1016/j.gaitpost.2004.01.010
8. Huang X, Xue Y, Ren S, Wang F. Sensor-Based Wearable Systems for Monitoring Human Motion and Posture: A Review. Sensors. 2023 Nov 8;23(22):9047. doi:10.3390/s23229047
9. Ahmad N, Ghazilla RAR, Khairi NM, Kasi V. Reviews on Various Inertial Measurement Unit (IMU) Sensor Applications. IJSPS. 2013;256–62. doi:10.12720/ijsps.1.2.256-262
10. Τσιβγούλης Στυλιανός (2011 Πανεπιστήμιο Κρήτης) Καταγραφή και ανάλυση κινησιομετρικών χαρακτηριστικών με στόχο την εκτίμηση του μυοσκελετικού συστήματος των αθλητών [Internet]. [cited 2025 Oct 16]. Available from: https://freader.ekt.gr/eadd/index.php?doc=23219&lang=el#p=33
11. Passaro VMN, Cuccovillo A, Vaiani L, De Carlo M, Campanella CE. Gyroscope Technology and Applications: A Review in the Industrial Perspective. Sensors (Basel). 2017 Oct 7;17(10):2284. doi:10.3390/s17102284 PubMed PMID: 28991175; PubMed Central PMCID: PMC5677445.
12. Kala R. An introduction to robotics. In: Autonomous Mobile Robots [Internet]. Elsevier; 2024 [cited 2025 Oct 16]. p. 1–48. Available from: https://linkinghub.elsevier.com/retrieve/pii/B9780443189081000108 doi:10.1016/B978-0-443-18908-1.00010-8
13. Movella DOT User Manual [Internet]. [cited 2025 Sep 28]. Available from: https://www.movella.com/hubfs/Movella%20DOT%20User%20Manual.pdf
14. Vitali RV, Perkins NC. Determining anatomical frames via inertial motion capture: A survey of methods. Journal of Biomechanics. 2020 Jun 9;106:109832. doi:10.1016/j.jbiomech.2020.109832

15. Filippeschi A, Schmitz N, Miezal M, Bleser G, Ruffaldi E, Stricker D. Survey of Motion Tracking Methods Based on Inertial Sensors: A Focus on Upper Limb Human Motion. Sensors. 2017 Jun;17(6):1257. doi:10.3390/s17061257

16. D'Alcala' ER, Voerman JA, Konrath JM, Vydhyanathan A. Xsens DOT Wearable Sensor Platform White Paper. 2021 Jan 20.

17. Challis JH. Quaternions as a solution to determining the angular kinematics of human movement. BMC biomed eng. 2020 Dec;2(1):5. doi:10.1186/s42490-020-00039-z

18. Ferraz F, Filho L, Souza-Pinto G, Iwaki L, An T, Cardoso M. A comparative study of the accuracy between two computer-aided surgical simulation methods in virtual surgical planning. Journal of Cranio-Maxillofacial Surgery. 2020 Dec 1;49. doi:10.1016/j.jcms.2020.12.002

19. Oostendorp H, Beun RJ, Diggelen J, Eijk RM, Houtkamp JM, Prüst HHAM, Melguizo MC, Spek ED, Wouters PJM. Human-Media Interaction.

20. Hamano F. Derivative of Rotation Matrix Direct Matrix Derivation of Well Known Formula [Internet]. arXiv; 2013 [cited 2026 Mar 24]. Available from: http://arxiv.org/abs/1311.6010 doi:10.48550/arXiv.1311.6010

21. Solà J. Quaternion kinematics for the error-state Kalman filter [Internet]. arXiv; 2017 [cited 2025 Nov 4]. Available from: http://arxiv.org/abs/1711.02508 doi:10.48550/arXiv.1711.02508

22. Carlton JS. Propeller Geometry. In: Marine Propellers and Propulsion [Internet]. Elsevier; 2019 [cited 2025 Nov 6]. p. 29–46. Available from: https://linkinghub.elsevier.com/retrieve/pii/B9780081003664000031 doi:10.1016/B978-0-08-100366-4.00003-1

23. Three-Dimensional Kinematics and Kinetics. In: Biomechanics and Motor Control of Human Movement [Internet]. John Wiley & Sons, Ltd; 2009 [cited 2026 Mar 20]. p. 176–99. Available from: https://onlinelibrary.wiley.com/doi/abs/10.1002/9780470549148.ch7 doi:10.1002/9780470549148.ch7

24. Pacher L, Chatellier C, Vauzelle R, Fradet L. Sensor-to-Segment Calibration Methodologies for Lower-Body Kinematic Analysis with Inertial Sensors: A Systematic Review. Sensors. 2020 Jun 11;20(11):3322. doi:10.3390/s20113322

25. Picerno P. 25 years of lower limb joint kinematics by using inertial and magnetic sensors: A review of methodological approaches. Gait Posture. 2017 Jan;51:239–46. doi:10.1016/j.gaitpost.2016.11.008 PubMed PMID: 27833057.

26. Bonfiglio A, Tacconi D, Bongers RM, Farella E. Effects of IMU sensor-to-segment calibration on clinical 3D elbow joint angles estimation. Front Bioeng Biotechnol. 2024 May 17;12:1385750. doi:10.3389/fbioe.2024.1385750

27. Ekdahl M, Loewen A, Erdman A, Sahin S, Ulman S. Inertial Measurement Unit Sensor-to-Segment Calibration Comparison for Sport-Specific Motion Analysis. Sensors. 2023 Jan;23(18):7987. doi:10.3390/s23187987

28. Picerno P, Cereatti A, Cappozzo A. Joint kinematics estimate using wearable inertial and magnetic sensing modules. Gait & Posture. 2008 Nov 1;28(4):588–95. doi:10.1016/j.gaitpost.2008.04.003

29. Bergamini E, Ligorio G, Summa A, Vannozzi G, Cappozzo A, Sabatini AM. Estimating Orientation Using Magnetic and Inertial Sensors and Different Sensor Fusion Approaches: Accuracy Assessment in Manual and Locomotion Tasks. Sensors. 2014 Oct;14(10):18625–49. doi:10.3390/s141018625

30. Sabatini AM. Estimating Three-Dimensional Orientation of Human Body Parts by Inertial/Magnetic Sensing. Sensors. 2011 Jan 26;11(2):1489–525. doi:10.3390/s110201489

31. Alatise MB, Hancke GP. Pose Estimation of a Mobile Robot Based on Fusion of IMU Data and Vision Data Using an Extended Kalman Filter. Sensors (Basel). 2017 Sep 21;17(10):2164. doi:10.3390/s17102164 PubMed PMID: 28934102; PubMed Central PMCID: PMC5676736.

32. Yun X, Bachmann ER. Design, Implementation, and Experimental Results of a Quaternion-Based Kalman Filter for Human Body Motion Tracking. IEEE Transactions on Robotics. 2006 Sep;22(6):1216–27. doi:10.1109/TRO.2006.886270

33. Sabatini AM. Quaternion-based extended Kalman filter for determining orientation by inertial and magnetic sensing. IEEE Transactions on Biomedical Engineering. 2006 Jul;53(7):1346–56. doi:10.1109/TBME.2006.875664

34. Majumder S, Deen MJ. Wearable IMU-Based System for Real-Time Monitoring of Lower-Limb Joints. IEEE Sensors Journal. 2021 Mar;21(6):8267–75. doi:10.1109/JSEN.2020.3044800

35. Subramaniam S, Majumder S, Faisal AI, Deen MJ. Insole-Based Systems for Health Monitoring: Current Solutions and Research Challenges. Sensors. 2022 Jan;22(2):438. doi:10.3390/s22020438

36. Höher J, Lischke B, Petersen W, Mengis N, Niederer D, Stein T, Stoffels T, Prill R, Schmidt-Lucke C. Sensor-based telerehabilitation system increases patient adherence after knee surgery. PLOS Digital Health. 2023;2(2):e0000175. doi:10.1371/journal.pdig.0000175

37. Cottrell MA, Galea OA, O'Leary SP, Hill AJ, Russell TG. Real-time telerehabilitation for the treatment of musculoskeletal conditions is effective and comparable to standard practice: a systematic review and meta-analysis. Clin Rehabil. 2017 Dec;31(5):625–38. doi:10.1177/0269215516645148 PubMed PMID: 27141087.

38. Faisal AI, Majumder S, Mondal T, Cowan D, Naseh S, Deen MJ. Monitoring Methods of Human Body Joints: State-of-the-Art and Research Challenges. Sensors. 2019 Jan;19(11):2629. doi:10.3390/s19112629

39. Jarallah M, Withers TM, Rosewilliam S, Stathi A, Greaves CJ. Methods for assessing exercise fidelity in unsupervised home-based cardiovascular rehabilitation: a scoping review. BMC Sports Sci Med Rehabil. 2025 Feb 28;17(1):31. doi:10.1186/s13102-025-01069-7

40. Komaris DS, Tarfali G, O'Flynn B, Tedesco S. Unsupervised IMU-based evaluation of at-home exercise programmes: a feasibility study. BMC Sports Sci Med Rehabil. 2022 Feb 19;14:28. doi:10.1186/s13102-022-00417-1 PubMed PMID: 35183244; PubMed Central PMCID: PMC8857882.

41. Tannous H, Istrate D, Perrochon A, Daviet JC, Benlarbi-Delai A, Sarrazin J, Ho Ba Tho MC, Dao TT. GAMEREHAB@HOME: A New Engineering System Using Serious Game and Multisensor Fusion for Functional Rehabilitation at Home. IEEE Trans Games. 2021 Mar;13(1):89–98. doi:10.1109/TG.2019.2963108

42. Han R, Lee BG, Pike M, Towey D, Yao Y, Wang Y, Chung WY. Sproutfit: an immersive seed-planting virtual reality game to enhance patient motivation for performing exercises for the prevention of venous

thromboembolism through loss and avoidance gamification. Virtual Reality. 2025 Aug 26;29(3):137. doi:10.1007/s10055-025-01220-2

43. Smits Serena R, Hinterwimmer F, Burgkart R, Von Eisenhart-Rothe R, Rueckert D. The Use of Artificial Intelligence and Wearable Inertial Measurement Units in Medicine: Systematic Review. JMIR Mhealth Uhealth. 2025 Jan 29;13:e60521. doi:10.2196/60521

44. Wei S, Wu Z. The Application of Wearable Sensors and Machine Learning Algorithms in Rehabilitation Training: A Systematic Review. Sensors. 2023 Sep 5;23(18):7667. doi:10.3390/s23187667

45. Trabassi D, Serrao M, Varrecchia T, Ranavolo A, Coppola G, De Icco R, Tassorelli C, Castiglia SF. Machine Learning Approach to Support the Detection of Parkinson's Disease in IMU-Based Gait Analysis. Sensors. 2022 May 12;22(10):3700. doi:10.3390/s22103700

46. Lin JJ, Hsu CK, Hsu WL, Tsao TC, Wang FC, Yen JY. Machine Learning for Human Motion Intention Detection. Sensors. 2023 Aug 16;23(16). doi:10.3390/s23167203

47. Chatzitofis A, Monaghan D, Mitchell E, Honohan F, Zarpalas D, O'Connor NE, Daras P. HeartHealth: A Cardiovascular Disease Home-based Rehabilitation System. Procedia Computer Science. 2015;63:340–7. doi:10.1016/j.procs.2015.08.352

48. Kim JY, Park G, Lee SA, Nam Y. Analysis of Machine Learning-Based Assessment for Elbow Spasticity Using Inertial Sensors. Sensors. 2020 Mar 14;20(6):1622. doi:10.3390/s20061622

49. Han Y, Liu X, Zhang N, Zhang X, Zhang B, Wang S, Liu T, Yi J. Automatic Assessments of Parkinsonian Gait with Wearable Sensors for Human Assistive Systems. Sensors. 2023 Feb 13;23(4). doi:10.3390/s23042104

50. Balletti N, Cascitelli A, Gabrieli P, Laudato G, Lazich A, Notarantonio M, Oliveto R, Ricciardi S, Scalabrino S, Simeone J. Virtual-Physio: A Virtual Assistant for Home Physiotherapy Rehabilitation.

51. Sumner J, Lim HW, Chong LS, Bundele A, Mukhopadhyay A, Kayambu G. Artificial intelligence in physical rehabilitation: A systematic review. Artif Intell Med. 2023 Dec;146:102693. doi: 10.1016/j.artmed.2023.102693

52. Da Gama A, Fallavollita P, Teichrieb V, Navab N. Motor Rehabilitation Using Kinect: A Systematic Review. Games Health J. 2015 Apr;4(2):123-35. doi: 10.1089/g4h.2014.0047

53. Zhang S, Li Y, Zhang S, Shahabi F, Xia S, Deng Y, Alshurafa N. Deep Learning in Human Activity Recognition with Wearable Sensors: A Review on Advances. Sensors (Basel). 2022 Feb 14;22(4):1476. doi: 10.3390/s22041476

54. Zaim T, Abdel-Hadi S, Mahmoud R, Khandakar A, Rakhtala SM, Chowdhury MEH. Machine Learning- and Deep Learning-Based Myoelectric Control System for Upper Limb Rehabilitation Utilizing EEG and EMG Signals: A Systematic Review. Bioengineering (Basel). 2025 Feb 3;12(2):144. doi: 10.3390/bioengineering12020144

55. Vakanski A, Jun HP, Paul D, Baker R. A Data Set of Human Body Movements for Physical Rehabilitation Exercises. Data (Basel). 2018 Mar;3(1):2. doi: 10.3390/data3010002

56. Sardari S, Sharifzadeh S, Daneshkhah A, Nakisa B, Loke SW, Palade V, Duncan MJ. Artificial Intelligence for skeleton-based physical rehabilitation action evaluation: A systematic review. Comput Biol Med. 2023 May;158:106835. doi: 10.1016/j.compbiomed.2023.106835

57. Palermo M, Mendes Lopes J, André J, Cerqueira J, Santos C. A multi-camera and multimodal dataset for posture and gait analysis (v1.0.0). PhysioNet 2021 RRID:SCR_007345. doi: 10.13026/fyxw-n385

58. Kasnesis P, Plavoukou T, Syropoulou AC, Toumanidis L, Georgoudis G. A Knee Rehabilitation Exercises Dataset for Postural Assessment using Wearable Devices. Sci Data. 2025 Apr 11;12(1):610. doi: 10.1038/s41597-025-04963-4

59. Li J, Xue J, Cao R, Du A, Mo S, Ran K. FineRehab: A Multi-modality and Multi-task Dataset for Rehabilitation Analysis, 2024 IEEE/CVF Conference on Computer Vision and Pattern Recognition Workshops (CVPRW), Seattle, WA, USA, 2024, pp. 3184-3193, doi: 10.1109/CVPRW63382.2024.00324

60. Li J, Zhang B, Tan X, Chen W, Liu Z, Zhang J, Huo W, Huang H, Liu L, Zhao X, K2MUSE: A human lower limb multimodal dataset under diverse conditions for facilitating rehabilitation robotics, arXiv:2504.14602, April 2025.

61. Nguyen AH, Nguyen HB, Le TTH, Nguyen CT, Thanh T, Nguyen H, Chu QT. RehabHand - A New Physical Rehabilitation Training Dataset: Construction and Benchmark Performances of the Relevant Hand Tasks. *IEEE Access* 2025, vol. 13, pp. 102373-102389, 2025, doi: 10.1109/ACCESS.2025.3578564

62. OpenCV - Open Computer Vision Library [Internet]. [cited 2025 Sep 28]. Available from: https://opencv.org/

63. NumPy [Internet]. [cited 2025 Sep 28]. Available from: https://numpy.org/

64. Matplotlib — Visualization with Python [Internet]. [cited 2025 Sep 28]. Available from: https://matplotlib.org/

65. pandas - Python Data Analysis Library [Internet]. [cited 2025 Sep 28]. Available from: https://pandas.pydata.org/

66. Kourtidis G., Physical Activity Data Acquisition and Processing via Inertial Sensor Networks, MSc Thesis, Master of Science in Biomedical Informatics, School of Medicine, Democritus University of Thrace, and ATHENA Research Center, Alexandroupoli, Greece, December, 2025. doi: 10.5281/zenodo.17404653

67. 55. Python documentation [Internet]. [cited 2025 Sep 28]. threading — Thread-based parallelism. Available from: https://docs.python.org/3/library/threading.html

68. Didaskalou S, Papageorgiou P, Tzatzimaki K, Liapi M, Portokallidis N, Drosatos G, Kaldoudi E. ThrombUS+ Study B2 Lower Limb Activity Data Collection Manual [Internet]. 2025 Apr 29 [cited 2025 Sep 2]. Available from: https://zenodo.org/records/16915308

69. Tzatzimaki K, Portokallidis N, Drosatos G, Kaldoudi E, Didaskalou S. A Comprehensive Infrastructure and Methodology for Multi-Modal Data Acquisition to Empower AI-Based Rehabilitation. In Proceedings of the 19th International Joint Conference on Biomedical Engineering Systems and Technologies, 2026, - Volume 3: HEALTHINF, ISBN 978-989-758-802-0, ISSN 2184-4305, pages 269-278. doi: 10.5220/0014351200004070

Appendix A: Software Installation and Configuration Guide

A.1. Source Code and Repository Access

The complete source code of the developed motion acquisition platform, including all necessary configuration files and dependency specifications, I hosted on GitHub. This repository serves as a centralized resource for version control and provides the latest updates to the software infrastructure. The project can be accessed and cloned via the following link:

GitHub Repository: https://github.com/thrombusplus/recording-studio

A.2. Environment Setup and Dependencies

The system is developed in Python 3.10+. Fo a successful deployment, it is recommended to create a virtual environment to manage the required libraries and avoid conflicts. The core dependencies, which ae also detailed in the repository's *requirements.txt* file, include:

- **Hardware Communication:** movelladot_pc_sdk (The official Movella DOT PC SDK must be installed/ linked to the Python environment to enable BLE communication and sensor synchronization)
- **Inertial Data and Math:** NumPy (1.26.4), Pandas (2.3.0)
- **Computer Vision:** OpenCV-python (4.11.0.86), Pillow (11.2.1)
- **Visualization and User Interface:** Matplotlib (3.10.3), Ipython (8.37.0)
- **Asynchronous Communication:** Asyncio (3.4.3), WebSocket (13.1)
- **Input Handling:** Pynput (1.8.1)

A.3. Hardware Requirements

To ensure the stable operation of the multi-threaded architecture and maintain the synchronized frame rate of 30 fps, the following hardware is required (according to XSens DOT User Manual [13]):

- **Processor (CPU)**: Intel Core i7 (10^{th} Gen) or equivalent
- **Memory (RAM)**: 32GB
- **Bluetooth 5.0 (or higher):** Essential for stable, concurrent BLE communication with six IMU sensors.
- **USB 3.0 Ports and extensions:** The system requires at least two dedicated USB 3.0 ports for the dual-camera system. To facilitate the required room positioning for axial and lateral views, active USB 3.0 extension cables are utilized to maintain high-bandwidth data transfer without signal degradation over distance.

Appendix B. Software Implementation Details

B.1. Automated data export and file naming logic

The following code segment implements the save_recording method, which orchestrates the final stage of the data acquisition pipeline. The primary function of this module is to ensure the systematic serialization of multimodal data into distinct file formats while maintaining strict naming conventions for data integrity.

```python
def save_recording(self, data_queue, imu_ordered_configuration, patient_id, exercise_name, pose_setting, label_ID):
    # Count existing recordings
    pattern = os.path.join(self.file_path, f"{patient_id}_{pose_setting}_{exercise_name}_{label_ID}_*")
    existing_files = glob.glob(pattern + ".csv")
    repeat_number = len(existing_files) + 1
    repeat_str = str(repeat_number).zfill(2)

    timestamp_str = time.strftime('%Y%m%d_%H%M%S')
    filename_base = f"{patient_id}_{pose_setting}_{exercise_name}_{label_ID}_{repeat_str}_{timestamp_str}"

    imu_csv_path = os.path.join(self.file_path, f"{filename_base}.csv")
    imu_txt_path = os.path.join(self.file_path, f"{filename_base}.txt")
    cam1_path = os.path.join(self.file_path, f"{filename_base}_camera1.mp4")
    cam2_path = os.path.join(self.file_path, f"{filename_base}_camera2.mp4")

    camera1_frames = []
    camera2_frames = []

    with open(imu_csv_path, mode='w', newline='') as csvfile, open(imu_txt_path, mode='w') as txtfile:
        writer = csv.writer(csvfile)

        # CSV header
        header = ["timestamp"]
        for i in range(6):
            header.append(f"IMU_{i}_sensor_ts")

        for i in range(6):
            header += [f"quat.w({i})", f"quat.x({i})", f"quat.y({i})", f"quat.z({i})"]
            header += [f"acc.x({i})", f"acc.y({i})", f"acc.z({i})"]
            header += [f"ang.x({i})", f"ang.y({i})", f"ang.z({i})"]
            header += [f"mag.x({i})", f"mag.y({i})", f"mag.z({i})"]

        writer.writerow(header)
```

Figure 21. Python implementation of the multimodal data storage logic. The code illustrates the *save_recording* method, which automates the generation of unique filenames based on experimental metadata (Patient ID, Pose, Exercise, Label) and system timestamps. While the displayed segment specifically details the structured initialization and header creation for .csv files, the same programming logic and naming convention are consistently applied for the generation of .txt and synchronized .mp4 files.

B.2. Sensor-to-segment calibration logic

The following code segment implements the static calibration outline this module is responsible for calculating the orientation offsets required to align the sensos' coordinate systems with the participant's anatomical frame at the beginning of each recording session.

```python
# Calibration reference = frame 0
self.visual_calibration_reference = {}
for i in range(6):
    col_q = [f"quat.w({i})", f"quat.x({i})", f"quat.y({i})", f"quat.z({i})"]
    if all(col in self.loaded_imu_data.columns for col in col_q):
        q_ref = self.loaded_imu_data.loc[0, col_q].values.astype(float)
        norm_sq = np.sum(q_ref ** 2)
        if not np.any(np.isnan(q_ref)):
            q_inv = np.array([q_ref[0], -q_ref[1], -q_ref[2], -q_ref[3]]) / norm_sq
            self.visual_calibration_reference[i] = q_inv
            logger.debug(f" IMU {i} reference saved from frame 0.")
        else:
            logger.warning(f" Invalid quaternion for IMU {i} in frame 0.")
```

Figure 22. Python implementation of the static calibration routine. This code automates the extraction of reference orientation from the initial frame (frame 0) for all six IMU sensors. The logic includes the calculation of the inverse quaternion using the squared norm to ensure numerical stability, establishing the anatomical coordinate offset required for subsequent kinematic normalization.